Solar Wind Statistical Relationships Useful for Providing Analysis Constraints and Additional Space Weather Data Products

Heather A. Elliott[1,2], and Nathalia Alzate[3]

(1) Southwest Research Institute, San Antonio, TX
(2) University of Texas in San Antonio, San Antonio, TX
(3) NASA Goddard Space Flight Center, Greenbelt, MD

helliott@swri.edu

Overview

Objectives:

1. Solar wind statistics constrain for the image inversions, models, & assimilations particularly for background wind.
2. Solar wind statistics useful for forecasting additional solar wind and IMF parameters, and geophysical indices.

Source Properties

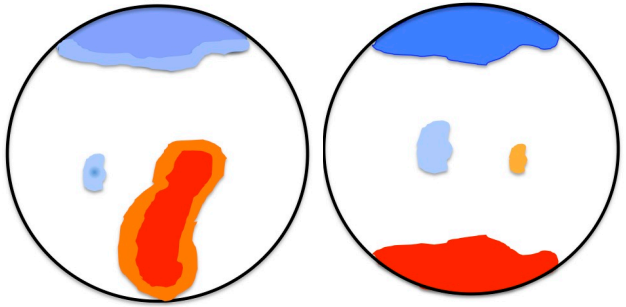

- Large polar coronal holes emit wind with speeds from 650 to 860 km/s.
- Moderately fast wind (450-650 km/s) from small low latitude coronal holes and/or from the edges of larger coronal holes.
- The slow wind (< 450 km/s) is more variable, cooler, more dense, and may have multiple sources (streamers and or edges of coronal holes).
- Dynamic interactions alter the solar wind properties en route.

Dynamic Interactions

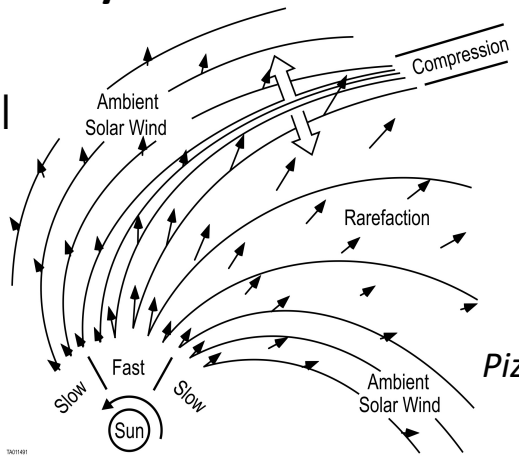

Pizzo, 1978

Dynamic Interactions and Source Properties

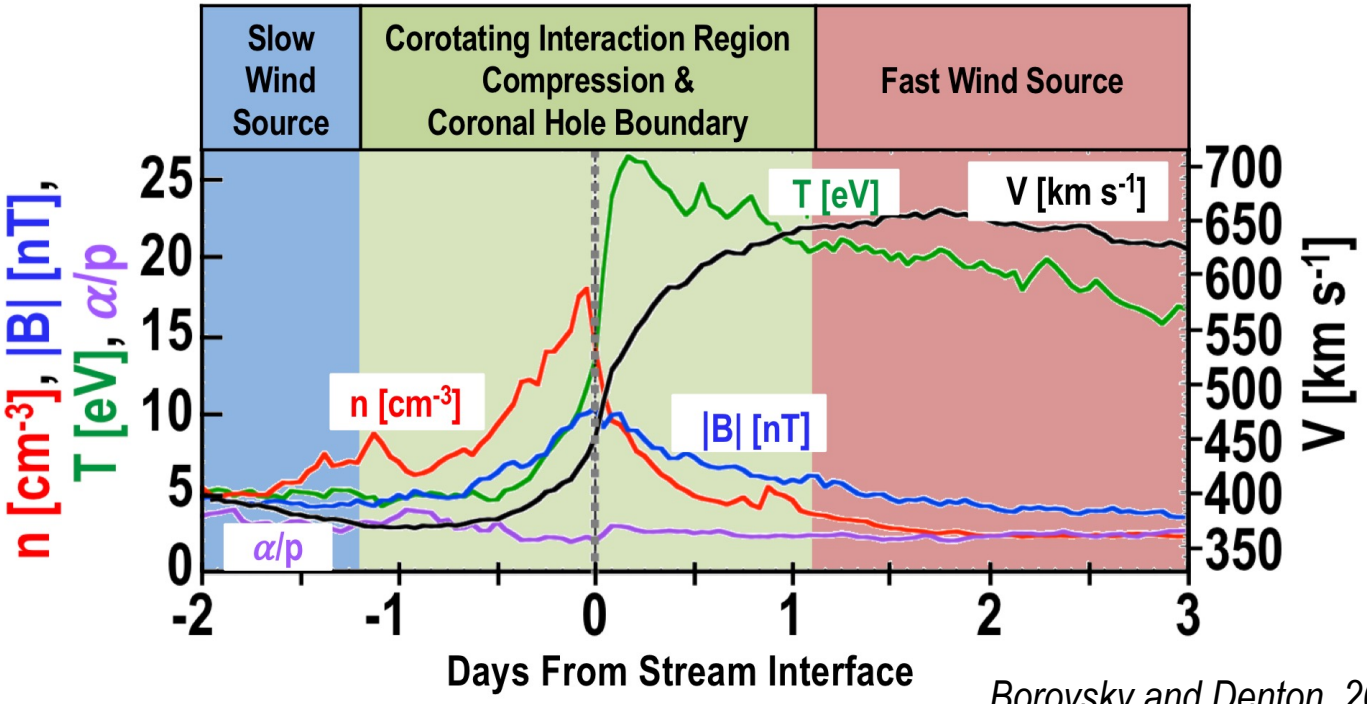

Borovsky and Denton, 2010

Superposed epoch analysis of 27 CIRs illustrates contributions of source properties and dynamic interactions, which produce correlations amongst solar wind and IMF parameters.

Using the Speed-Time Slope To Reveal Radial Variation of Dynamic Interactions

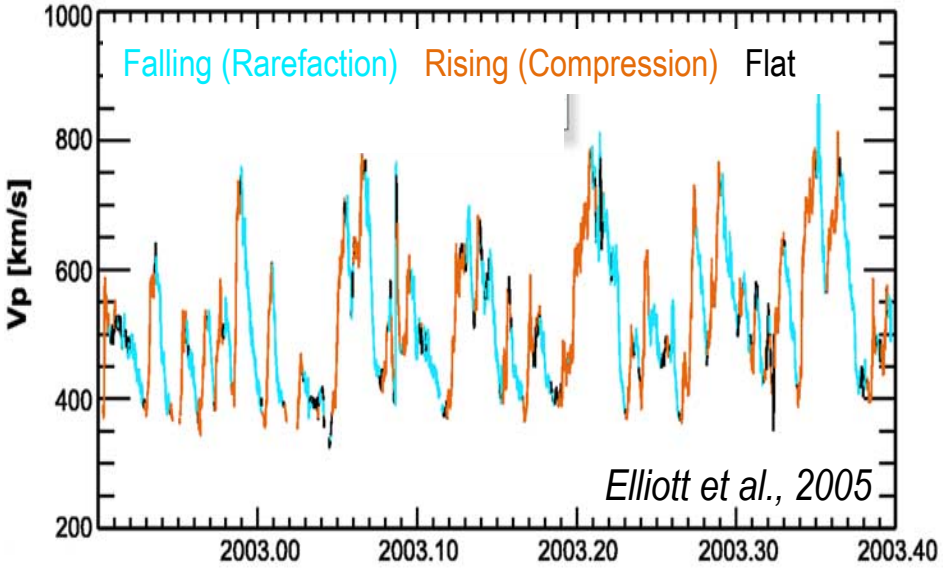

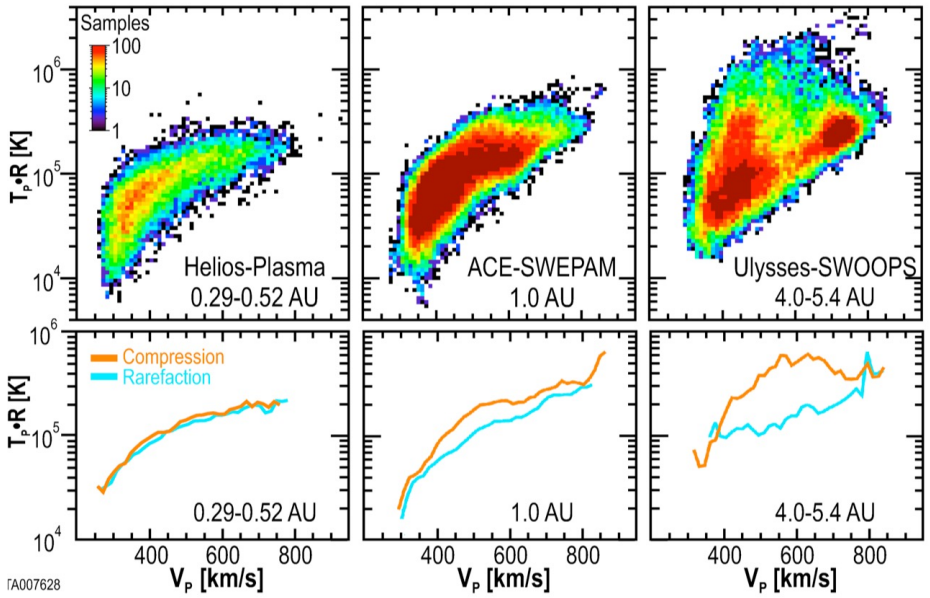

Elliott et al., 2012

We can use the steepness (dV/dt) of the rise and fall of the solar wind speed profile to identify compressions (rising) and rarefactions (falling).

Density Radial Profile Nearly Spherical Expansion

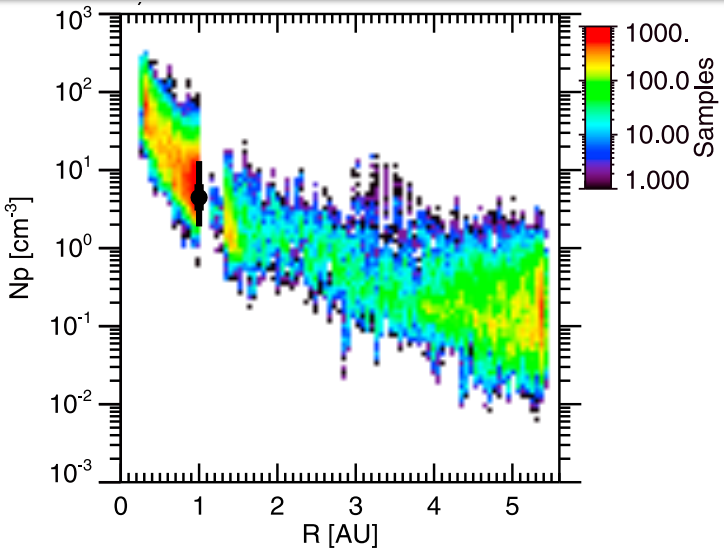

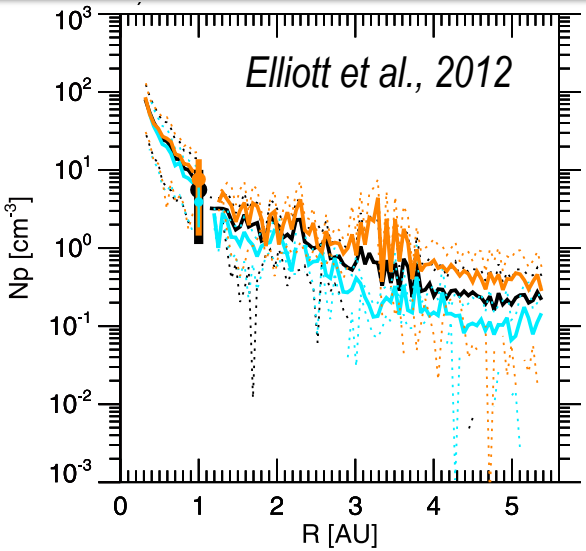

Table 1. List of Exponents From Power Law Fits to Ulysses and Helios Solar Wind Parameters Versus Radial Distance *Elliott et al., 2012*

Parameter	All	Compression	Rarefaction	Low Latitude or Polar Coronal Holes
T	0.72	0.50	0.81	Low Latitude
n	2.25	2.00	2.51	Low Latitude
ϵ	1.64	1.40	1.70	Low Latitude
T	1.01	0.80	1.08	Polar Coronal Hole
n	1.78	1.48	1.98	Polar Coronal Hole
ϵ	2.03	1.81	2.09	Polar Coronal Hole

- The density generally decreases at the spherical expansion (r^{-2}).
- Dynamic interactions cause some of the slight deviations from spherical expansion (r^{-2}).

- Even over the poles and in the outer heliosphere (Elliott et al., 2016;2019) the density decreases at nearly the spherical expansion rate.

T-V Relationship

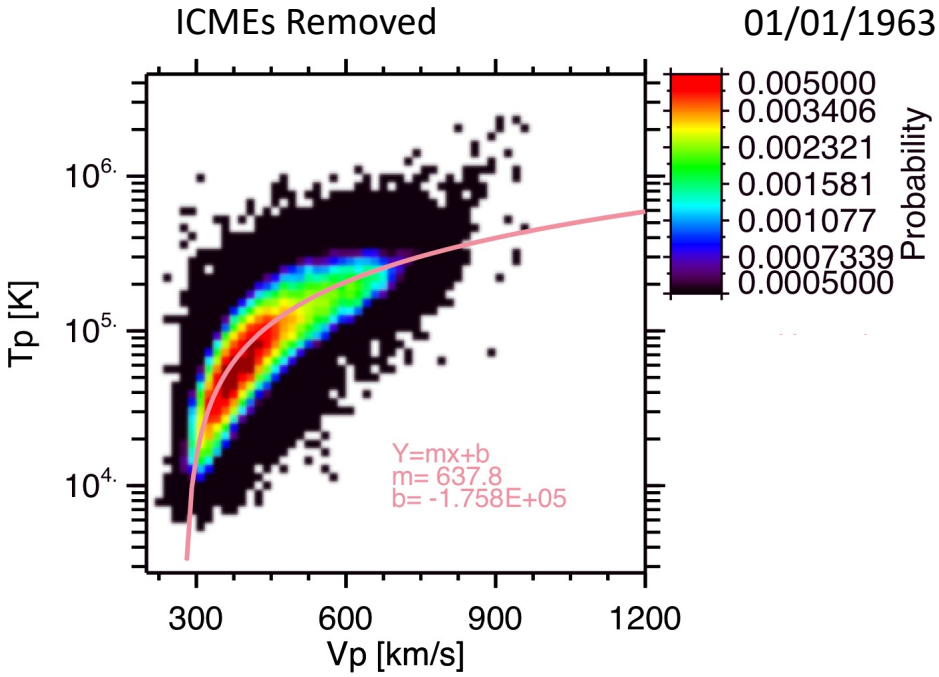

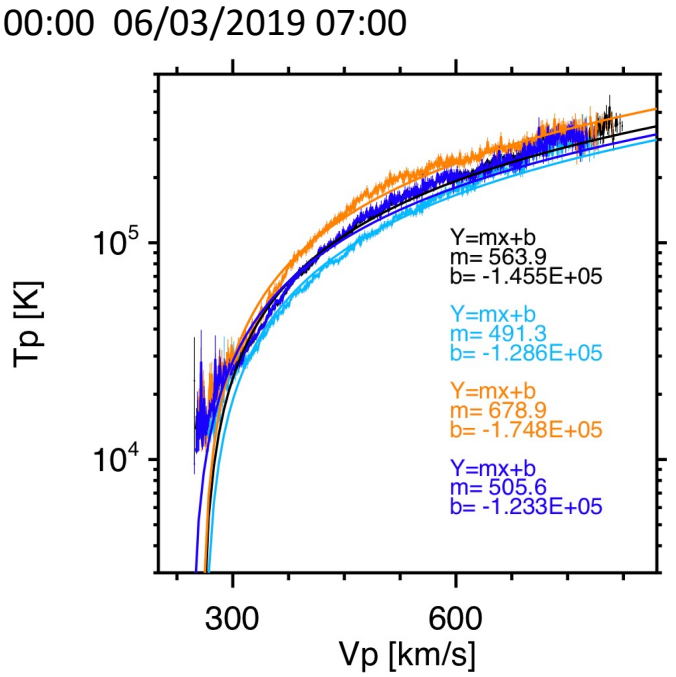

- **Linear** relationship between T and V.
- Sorting by the 2-day average of $\langle dV/dt \rangle_{2day}$ improves the ability to reproduce T and V.

- Rising profiles (orange) $\langle dV/dt \rangle_{2day} > 7000$km/s/year
- Falling profiles (light blue) $\langle dV/dt \rangle_{2day} < -7000$km/s/year
- Flat profiles (dark blue) $|\langle dV/dt \rangle_{2day}| \leqq 7000$km/s/year
- All the data (black)

n-V Relationship

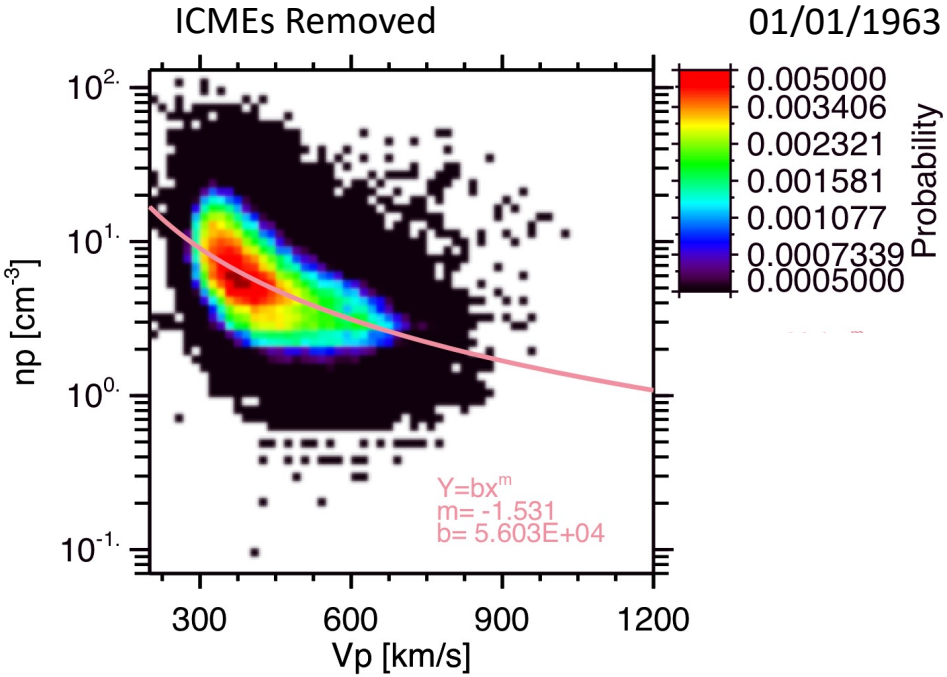

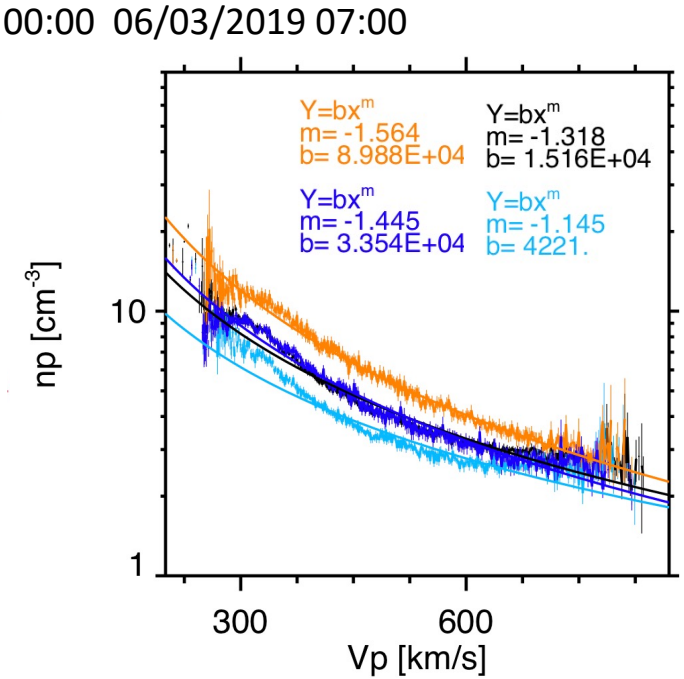

- **Power Law** relationship between n and V.
- Sorting by the 2-day average of $\langle dV/dt \rangle_{2day}$ improves the ability to reproduce T and V.

- Rising profiles (orange) $\langle dV/dt \rangle_{2day} > 7000$km/s/year
- Falling profiles (light blue) $\langle dV/dt \rangle_{2day} < -7000$km/s/year
- Flat profiles (dark blue) $|\langle dV/dt \rangle_{2day}| \leqq 7000$km/s/year
- All the data (black)

Many Quantities Have Long Term Trends; Baselines for Some Constraints Need to Be Updated to Account for These

- A constant number flux is a commonly used constraint.
- Other common constraints are an r^{-2} profile is for n and Br.

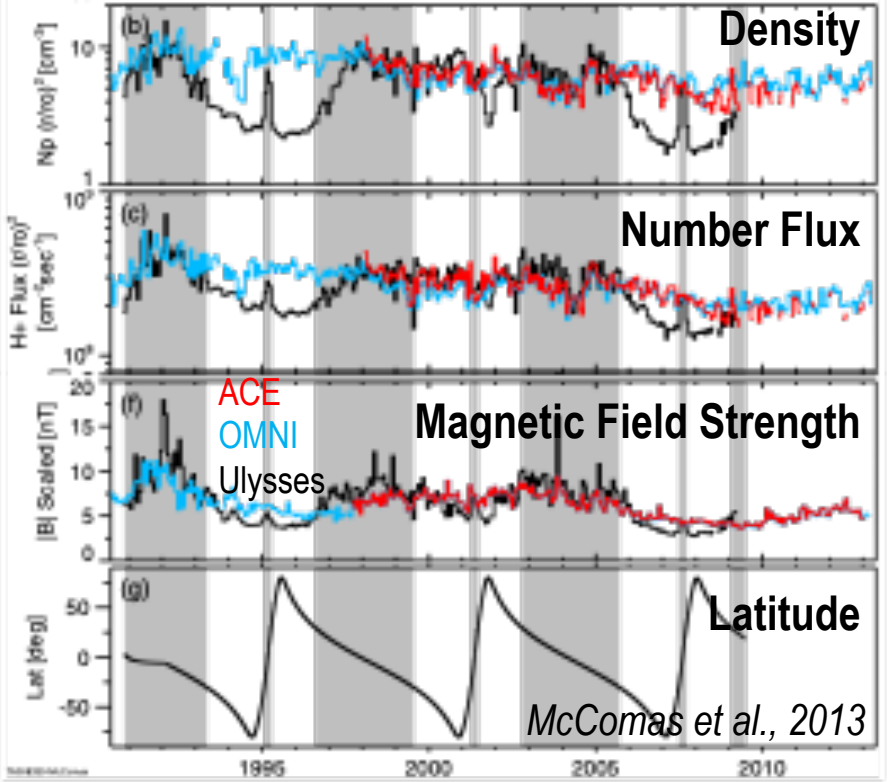

- Long-term baseline time variations need to be accounted for by adjusting the baseline for some radial trends.

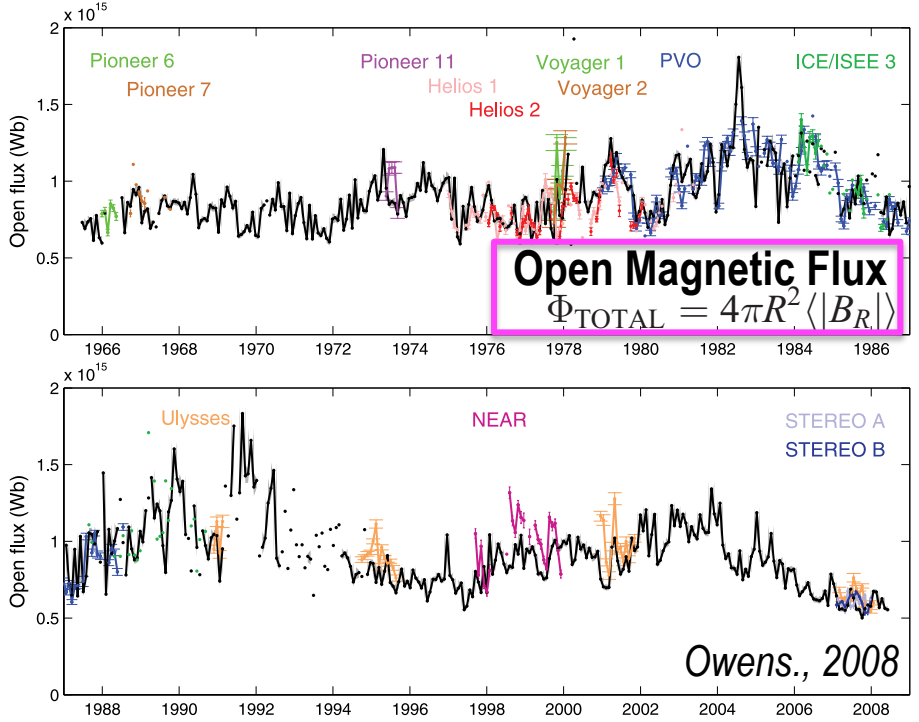

$|B|/\langle|B|\rangle_{PR}$ vs. $\langle dV/dt\rangle$

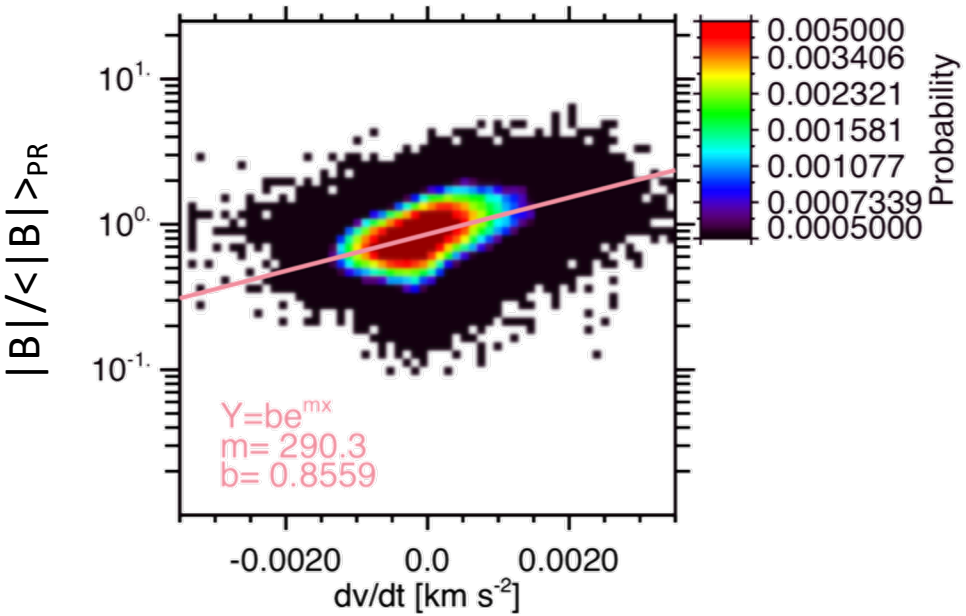

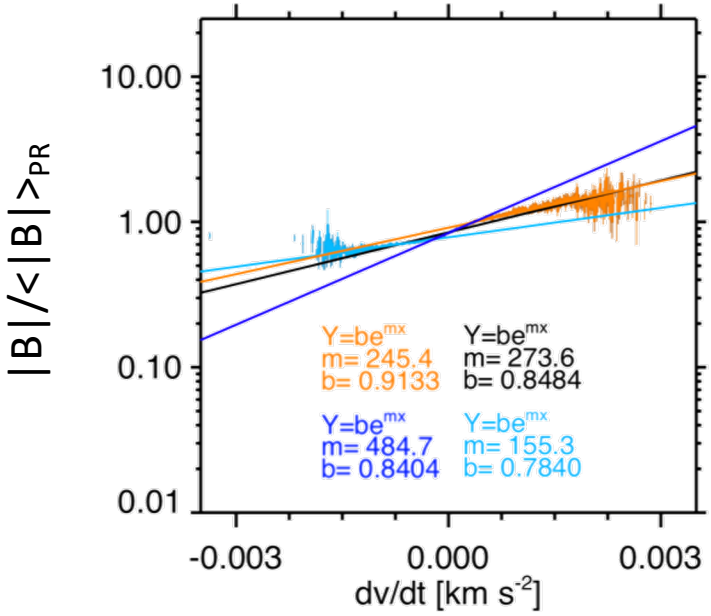

- Normalize interplanetary magnetic field strength (|B|) by the average value over the prior solar rotation to remove most of the very long term trends (solar cycle and greater) present in |B|.
- $|B|/\langle|B|\rangle_{prior\ rot}$ is plotted vs $\langle dV/dt\rangle_{2day}$ since we know that |B| typically peaks when in the middle of the rise in speed.

Radial Profile of the Radial Component (Br) of the IMF

- The radial component of the IMF drops off sharply with distance in the inner heliosphere as the solar wind expands and carries with IMF with it.
- ADAPT-WSA estimates Br at the source surface.
- $B_r \propto r^{-2.00}$
- Scale by a factor of 2 to account for systematic offset in Br (Linker et al., 2013).
- This is nearly the same assuming the distance is about 2 Rs shorter than anticipated.

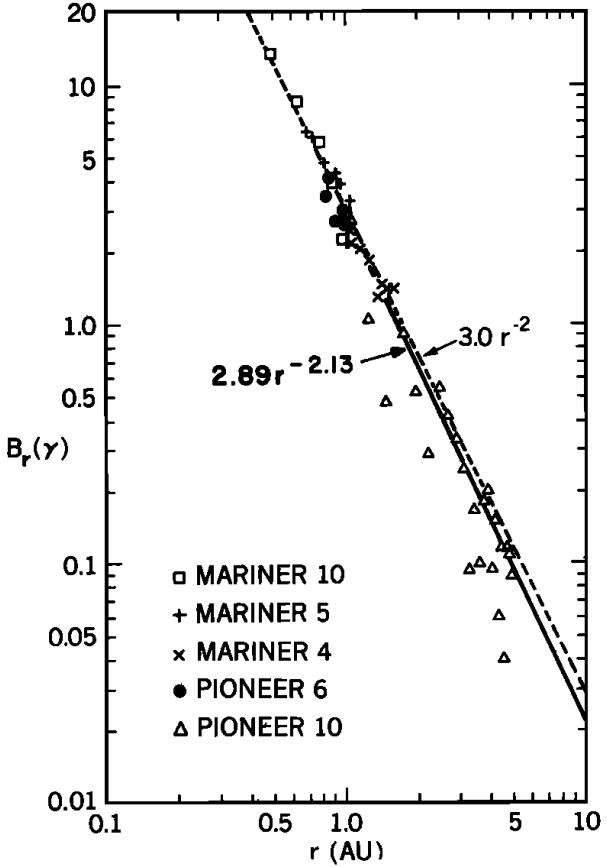

Bahannon et al., 1978

IMF BT & BN, and Conversion to GSM

- Parker Spiral
- $\phi_P = \text{atan}^{-1}\left(\left(v_\phi - \Omega r\cos\delta\right)/v_r\right)$
- $\phi_B = \phi_P$ for outward polarity and $\phi_B = 180^\circ + \phi_P$ for inward polarity
- B_T using $tan(\phi_B) = \frac{B_T}{B_R}$

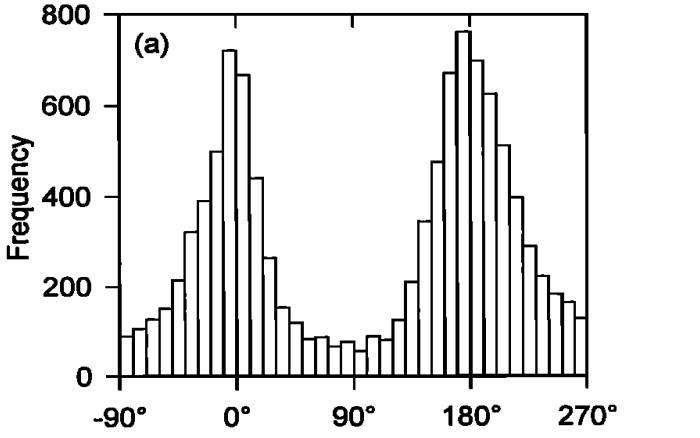

Forsyth et al., 1996

- Added a % of |B| to BR and BT to obtain compression effect.

  $B_R = B_R*(0.12)*|B|$ $B_T = B_T*(0.11)*|B|$
- B_N magnitude is then determined by solving

$$|B| = \sqrt{(B_T)^2 + (B_R)^2 + (B_N)^2}$$

- Transform from RTN to GSM.
- For a given polarity (Br sign) look up the sign for Bz using the time of day and DOY.

Russell-McPherron Effect

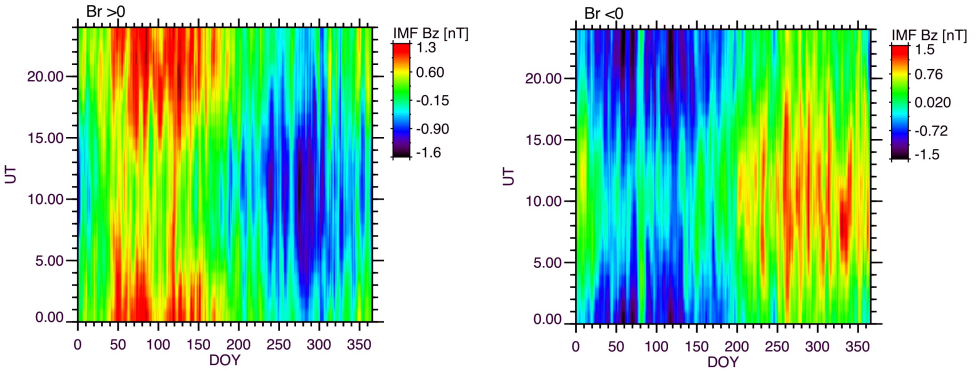

Forecasting Kp Index

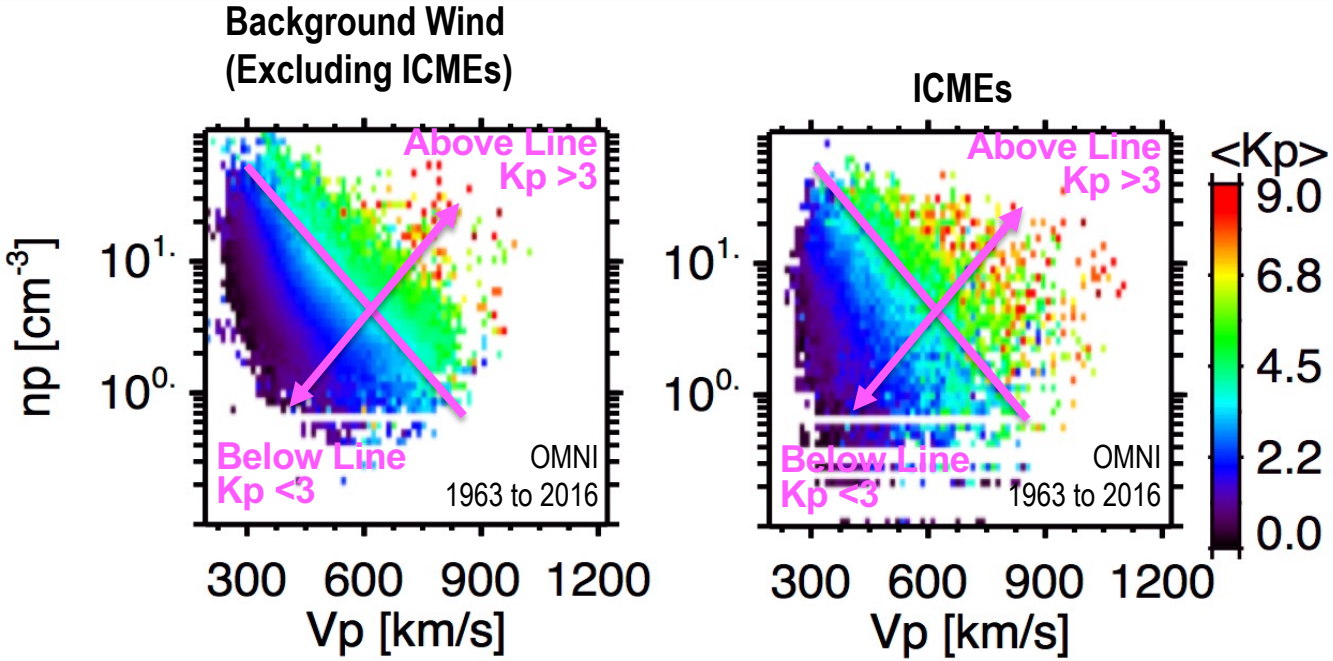

Kp Index
Lookup table of Kp binned by both n_p & V_p

- To determine if Kp is high or low, you only need to determine if V and n (or another measure compression e.g. dV/dt) are high or low.
- CME tracking the imaging that includes polarization information such that both n and V can be determined.

Wang-Sheeley-Arge Speed Formula

$$v_{\mathrm{wsa}}(f_{\mathrm{p}}, d; v_0, v_1, \beta, \gamma, w, \delta) = v_0 + \frac{v_1 - v_0}{(1 + f_{\mathrm{p}})^{\alpha}} \cdot \left\{ \beta - \gamma \cdot \exp[-(d / w)^{\delta}] \right\}^3$$

(Reiss et al., 2019)

Dependent Variables:

- *fp* -expansion factor
- d - angle to the open-closed field line boundary (~ angle to coronal hole boundary)
- Other qua.ntities are constants/fit parameters

Detailed Analysis of Residual Errors Before and After Correcting

- In each row the residual speed errors are analyzed three ways: 1) vs. fp and d, 2) vs. d and V, & 3) vs. fp and V.
- The top row are the residual errors for the ADAPT-WSA model.
- Bottom row shows residual errors after correcting the ADAPT-WSA model using the residual error array vs. fp & d in (a).

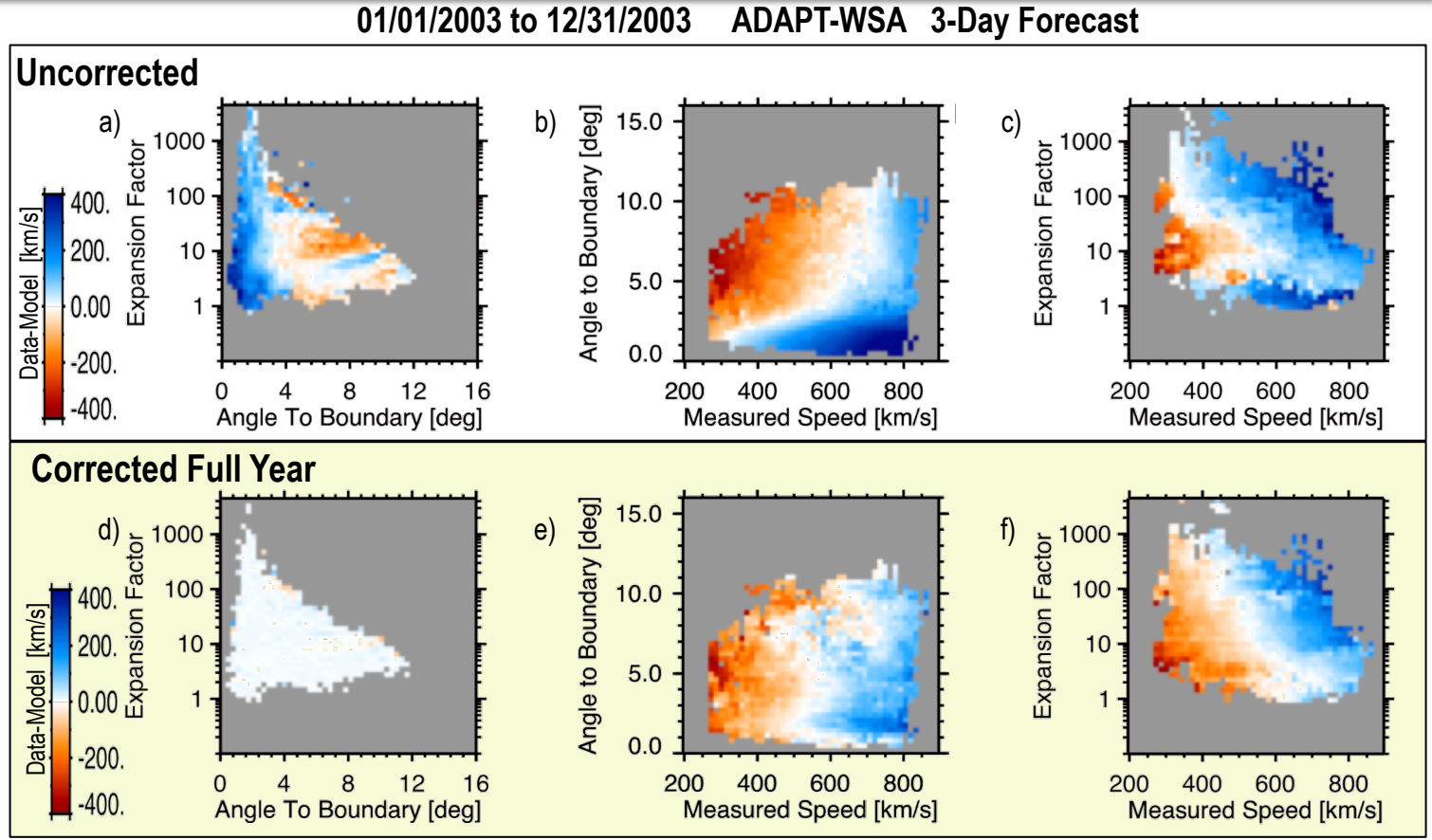

Overview of Residual Errors With and Without Corrections

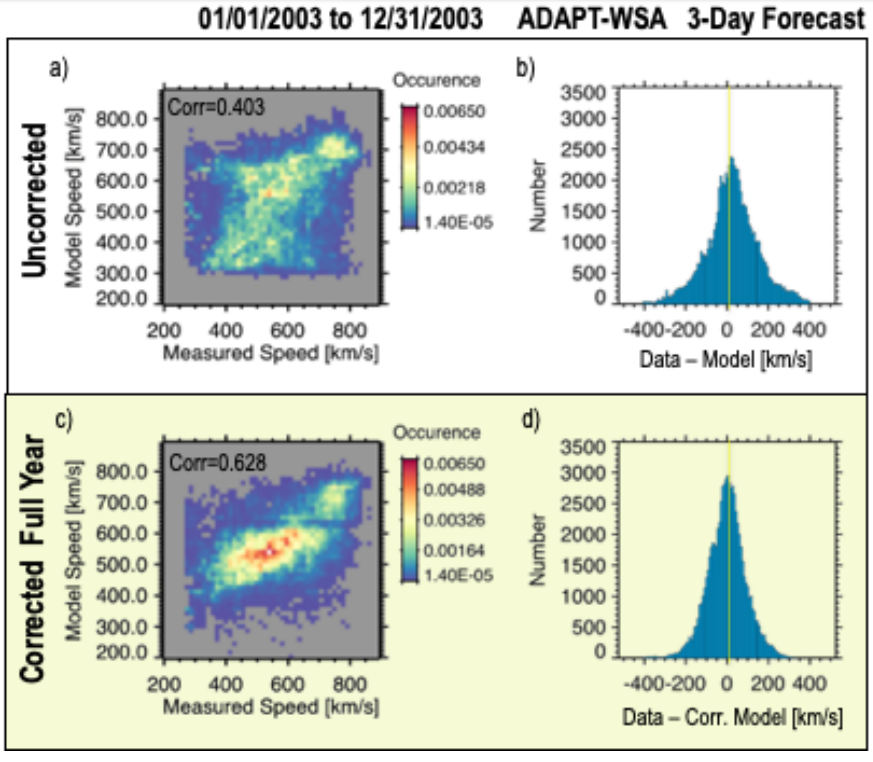

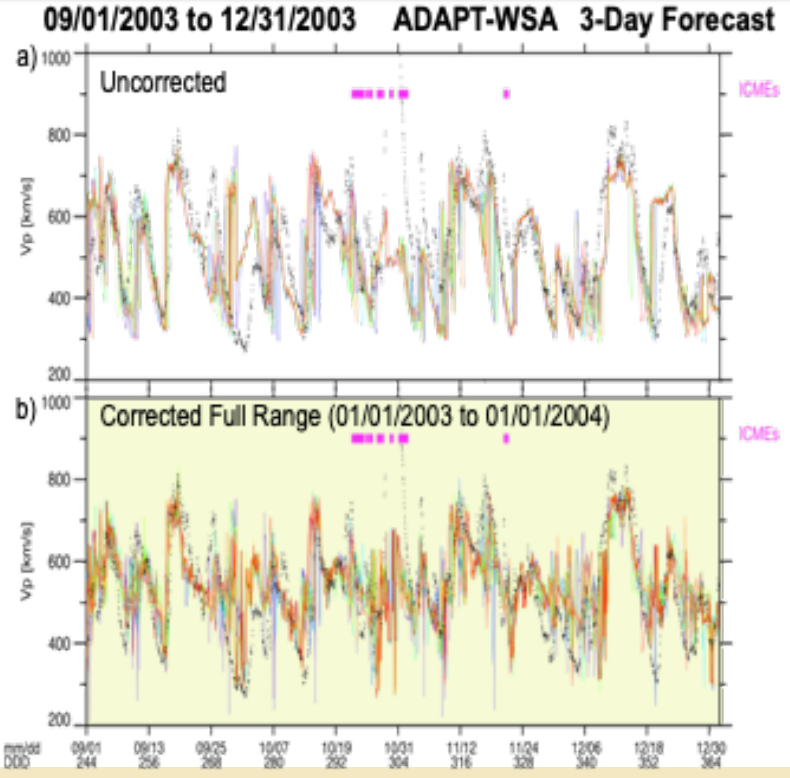

- Left: Overall comparison between ADAPT-WSA (top) and corrected ADAPT WSA speeds (bottom) vs. the measured speed, and residual error histograms.
- Right: Comparison of solar wind time series (black) with the model and corrected model results over-plotted (rainbow).

Example of Forecast Using ADAPT-WSA Corrected & Statistical Relationships

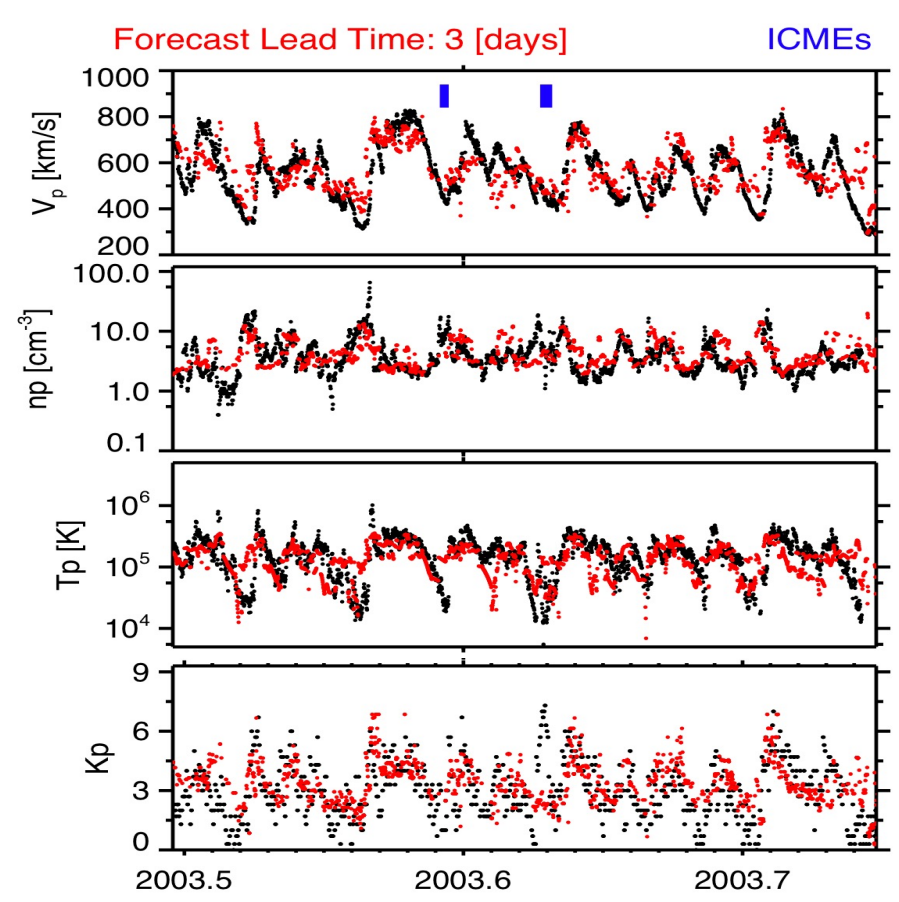

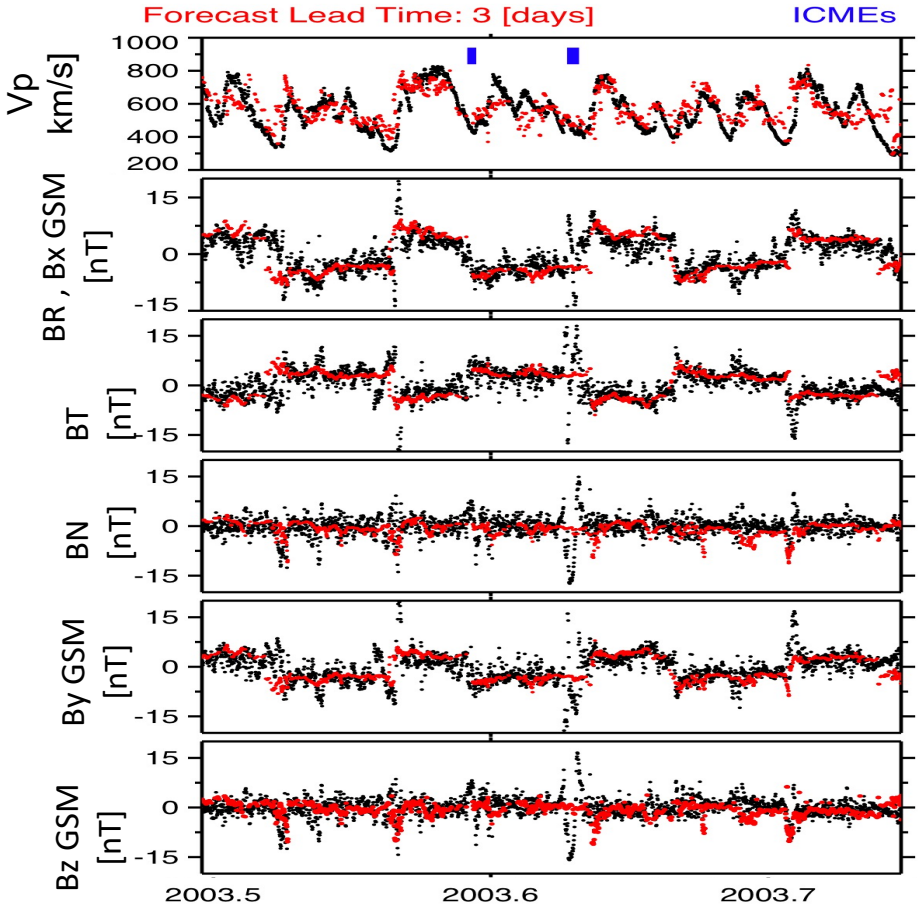

Using Tomography and Current Sheet Source Surface

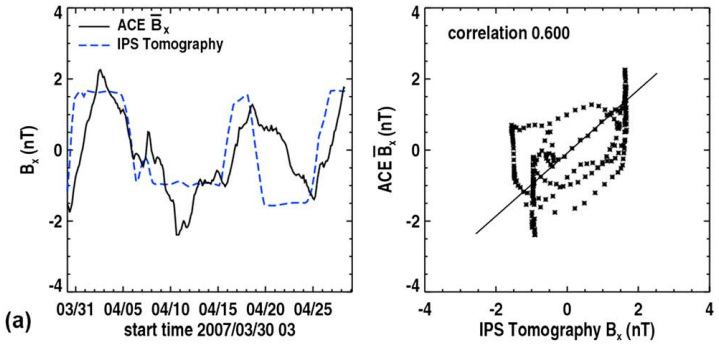

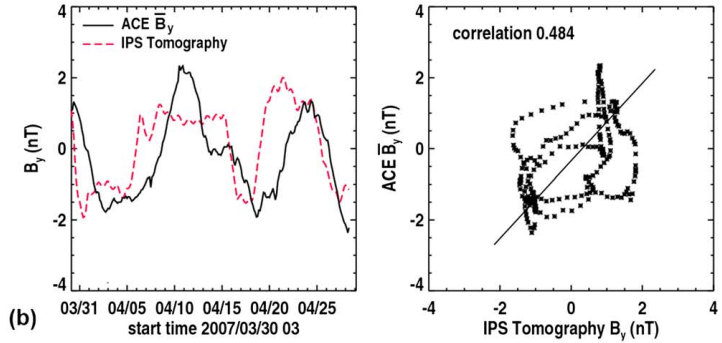

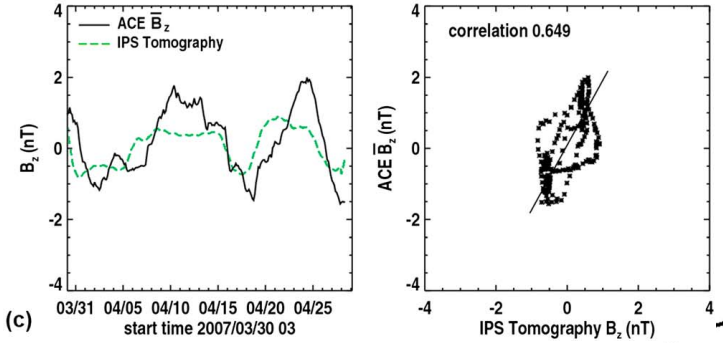

Jackson et al. 2019

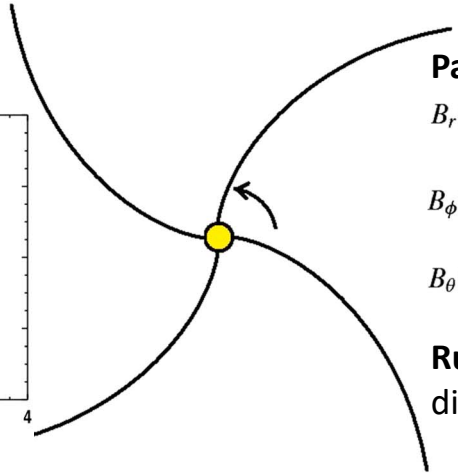

Parker Spiral

$$B_r(r,\phi,\theta) = B(r_0,\phi_0,\theta_0)\left(\frac{r_0}{r}\right)^2$$

$$B_\phi(r,\phi,\theta) = -B(r)\left(\frac{\omega r_0 \sin(\theta)}{V}\right)\left(\frac{r_0}{r}\right)$$

$$B_\theta(r,\phi,\theta) = 0$$

Russell-McPherron Effect: Tangential field direction tilt of the dipole.

Knowing the Statistical Trends For the Background Wind Can Improve CME Density Estimates

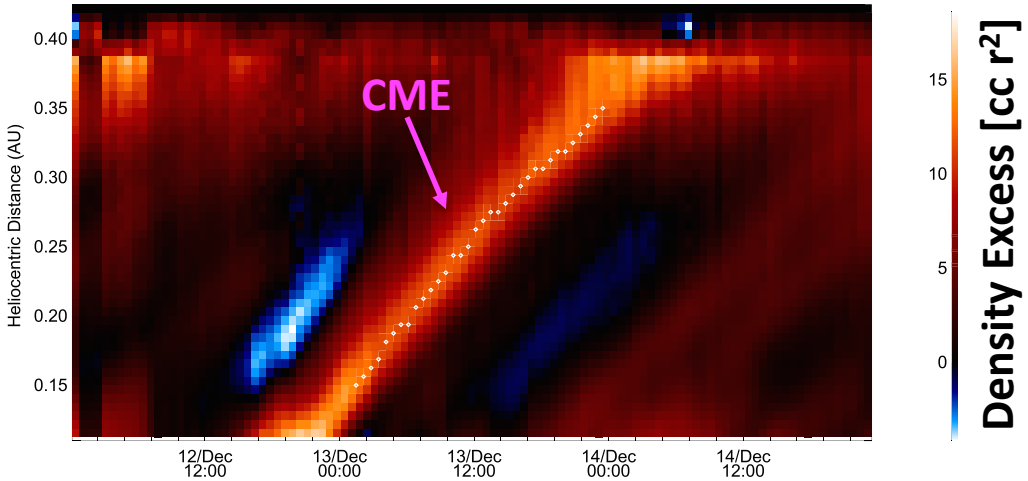

Figure 7. Density as a function of time and heliocentric distance. The figure is produced by taking the density along the Sun-Earth line from the tomographic reconstruction at each of the 108 time steps and stacking them consecutively. The overplotted diamonds show the peak in CME density at each of the time steps for which there existed a distinct density enhancement.

- Tracking the excess density relative to the K-corona.

Barnes, 2020

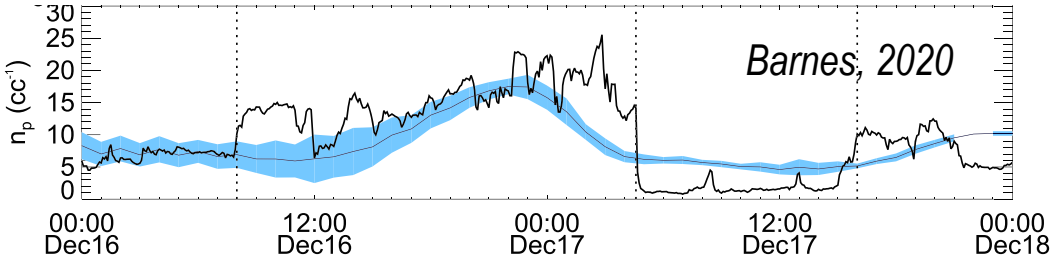

- To forecast the solar wind density of the CME a background solar wind density profile was added.

Summary

- Solar wind statistics can provide constraints for the image inversions particularly for the background wind.
- We can estimate more background solar wind and IMF parameters directly from solar wind speed –time profiles in the Earth direction
  - Forecast the solar wind density, temperature, field strength, and IMF (Bx, By, and Bz).
  - The speed and direction may be even more important than determining the solar wind density.
  - We need ways to utilize and integrate PUNCH data with other data sets in order to provide space weather forecasts such as to assimilations, tomography, inversions, and models constrained with imaging and solar wind statistical relationships such as those developed by Jackson et al, 2019, 2020, 2016 .
- Knowing the background wind trends can even be useful for helping to improve the tracking and density estimates for the CMEs.
- Search for statistical relationships between other the solar wind parameters and the the change in the density and speed as a function of distance that might be more directly related to PUNCH measurements.

END

helliott@swri.edu

Solar Wind Properties at 1 au Depend On A Combination of Source Properties and Dynamic Interactions

- Large polar coronal holes emit wind with speeds from 650 to 860 km/s.
- Moderately fast wind (450-650 km/s) from small low latitude coronal holes and/or from the edges of larger coronal holes.
- The slow wind (< 450 km/s) is more variable, cooler, more dense, and may have multiple sources (streamers and or edges of coronal holes).
- Dynamic interactions alter the solar wind properties en route.

Source Properties

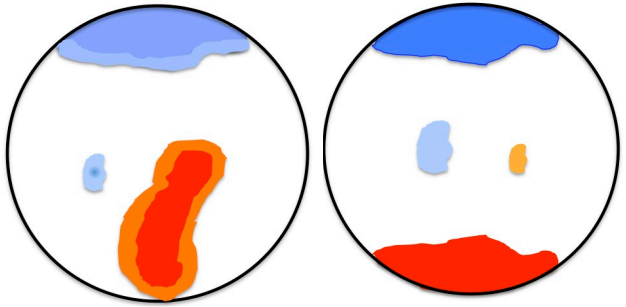

Dynamic Interactions

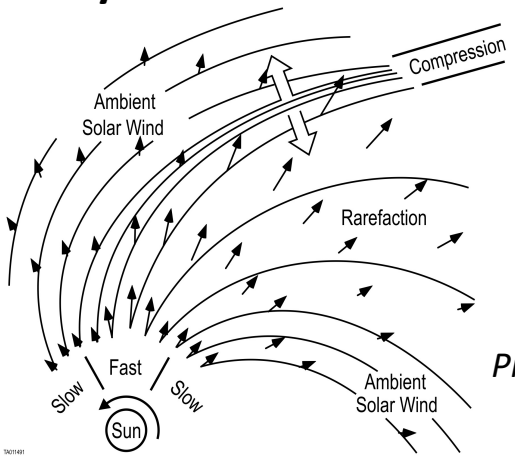

Pizzo, 1978

Identifying Dynamic Interactions

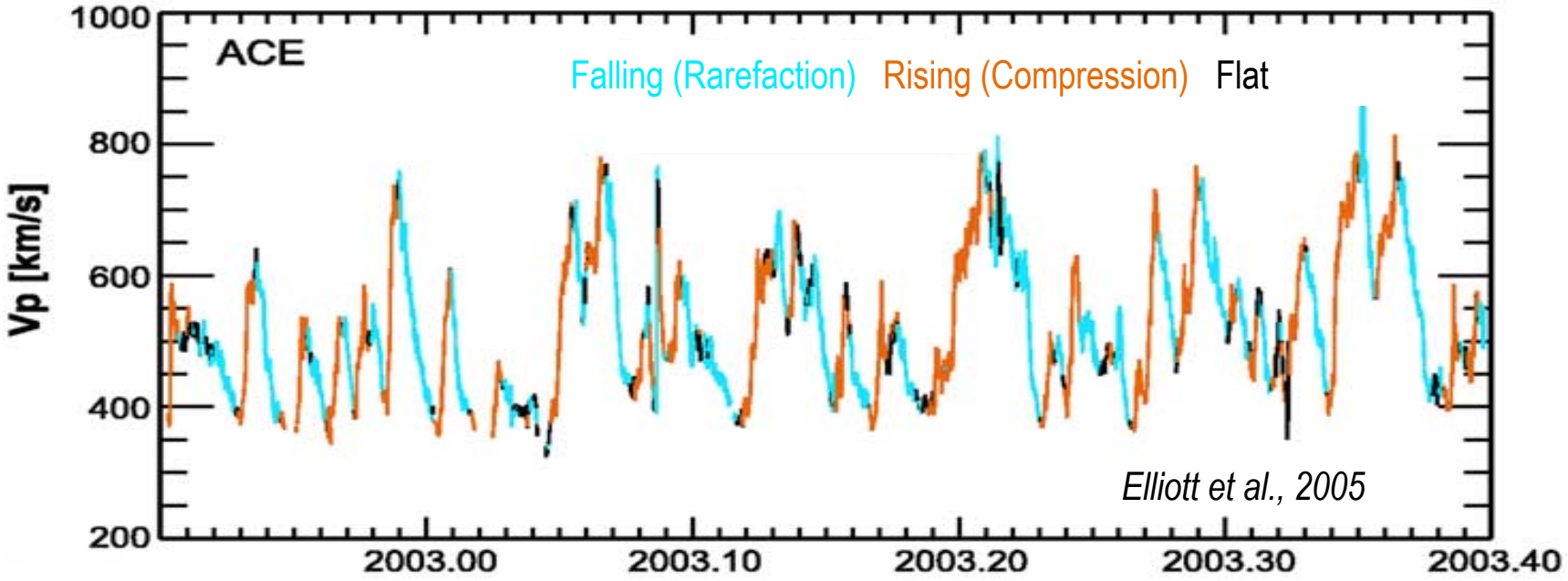

We can use the steepness (dV/dt) of the rise and fall of the solar wind speed profile to identify compressions (rising) and rarefactions (falling).

Formula Adjustments to Forecast Using Corrected ADAPT-WSA Speeds

Forecast Quantity	Original Formula	Adjusted Formula
V	V from ADAPT-WSA	V=V + correction from Figure 1
T when $\langle dV/dt \rangle_{2day} > \Gamma$	T=678.9V-1.749E5	T=678.9V-1.749E5
T when $\lvert\langle dV/dt \rangle_{2day}\rvert < \Gamma$	T=505.6V-1.233E5	T=505.6V-1.233E5
T when $dV/dt_{2day} < -\Gamma$	T=491.3V-1.286E5	T=491.3V-1.996E5
n when $dV/dt_{2day} > \Gamma$	$n=8.988E4V^{-1.564}$	$n=1.702E5V^{-1.584}$
n when $\lvert\langle dV/dt \rangle_{2day}\rvert < \Gamma$	$n=3.354E4\ V^{-1.445}$	$n=3.622E4V^{-1.458}$
n when $dV/dt_{2day} < -\Gamma$	$n=4.221E3V^{-1.145}$	$n=4.760E3V^{-1.179}$
$\lvert B\rvert$ when $dV/dt_{2day} > \Gamma$	$\lvert B\rvert = 0.9133\langle B \rangle_{pr} \exp(245.4\langle dV/dt \rangle)$	$\lvert B\rvert = 1.0033\langle B \rangle_{pr} \exp(255.4\langle dV/dt \rangle)$
$\lvert B\rvert$ when $\lvert\langle dV/dt \rangle_{2day}\rvert < \Gamma$	$\lvert B\rvert = 0.8404\langle B \rangle_{pr} \exp(482.7\langle dV/dt \rangle)$	$\lvert B\rvert = 0.8404\langle B \rangle_{pr} \exp(482.8\langle dV/dt \rangle)$
$\lvert B\rvert$ when $dV/dt_{2day} < -\Gamma$	$\lvert B\rvert = 0.7840\langle B \rangle_{pr} \exp(155.3\langle dV/dt \rangle)$	$\lvert B\rvert = 0.7040\langle B \rangle_{pr} \exp(145.3\langle dV/dt \rangle)$
B_R	B_R	$B_R = 1.3 \cdot \log_{10}(\lvert B\rvert)$
Kp	Lookup V value	Lookup : $V = V + 230 \cdot \log_{10}(V/640)$
	Lookup n value	Lookup: $n = n + 3.5 \cdot \log_{10}(n/2.7)+1$

- Above we show the formulas and adjustments made for the corrected ADAPT-WSA forecasts.
- **Γ=7000km/s/year**
- Optimizing through iteration (by hand) we only needed to slightly adjust the formulas to produce n, V, T, |B|, and Kp forecasts when we used the corrected ADAPT-WSA speeds.

Forecast Test On Full Year (Scalar Quantities)
Using Corrected Speeds and Adjusted Formulas

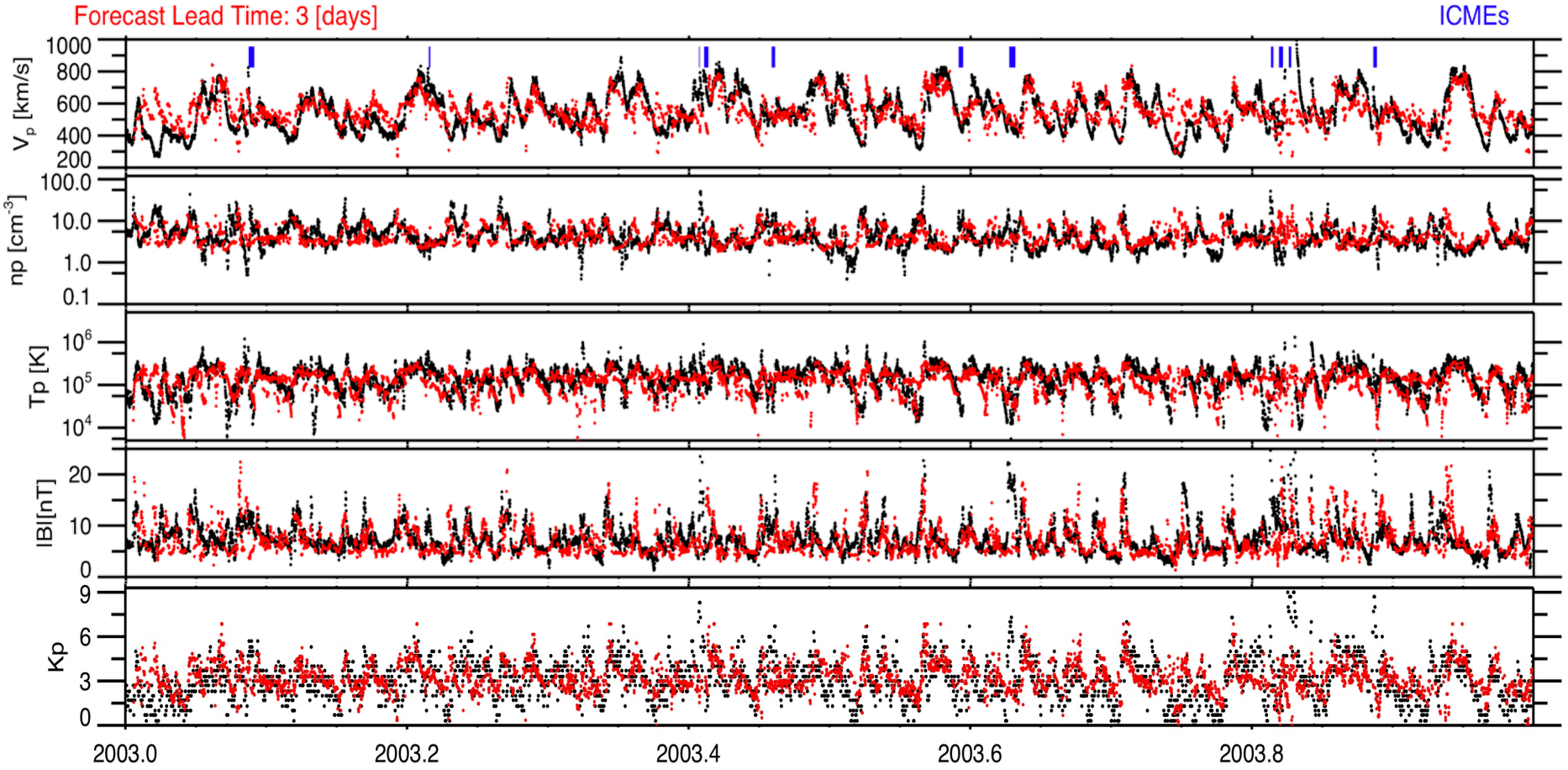

Forecast Test On Full Year (IMF)
Using Corrected Speeds and Adjusted Formulas

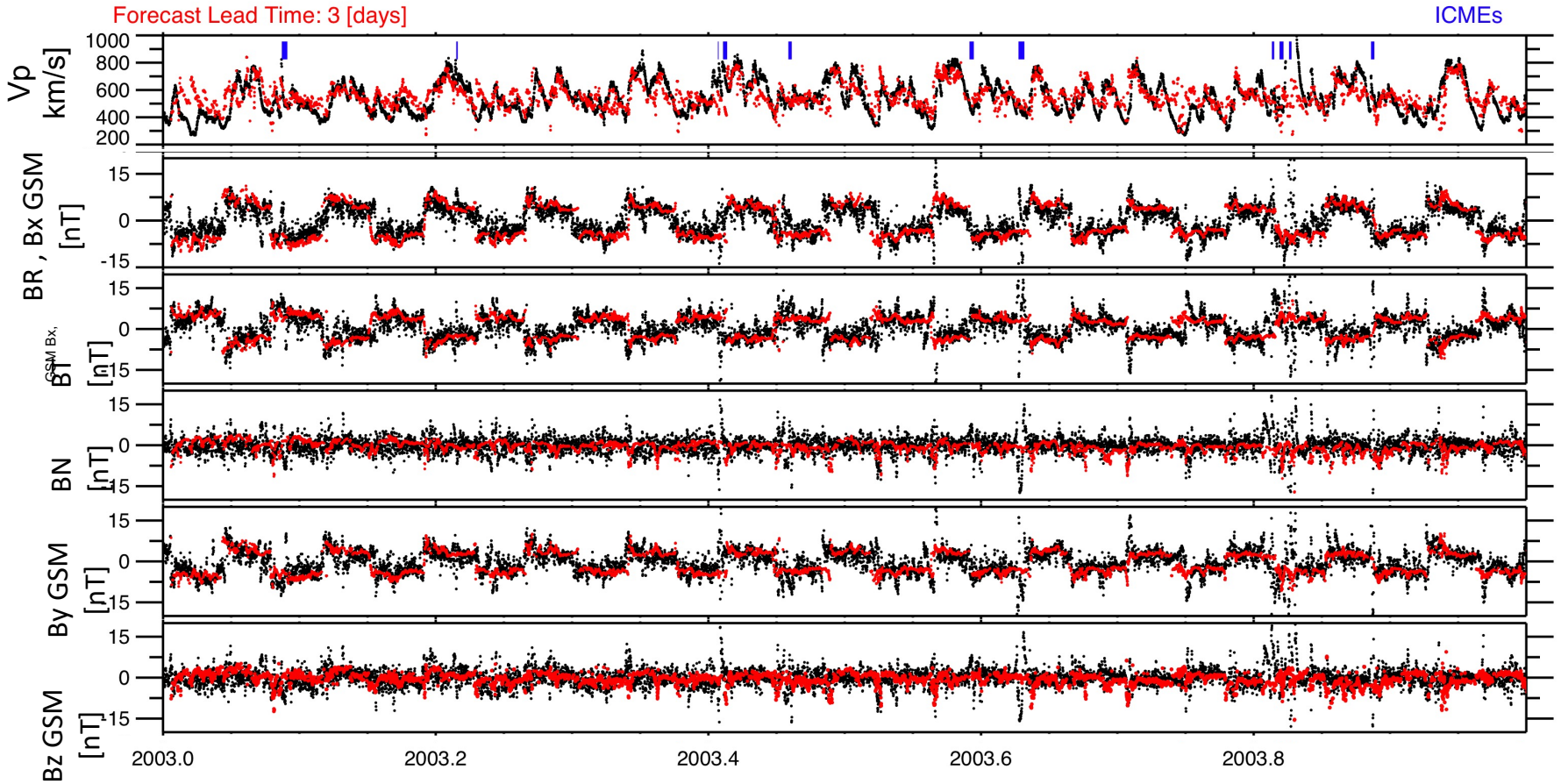

Determining |B| vs <dV/dt>$_{2day}$

- Compared |B| to the a running estimate of dV(t)/dt in a 2day window.
- The exponential fit parameters for each year of |B| vs. dV/dt do not show a systematic time variation.

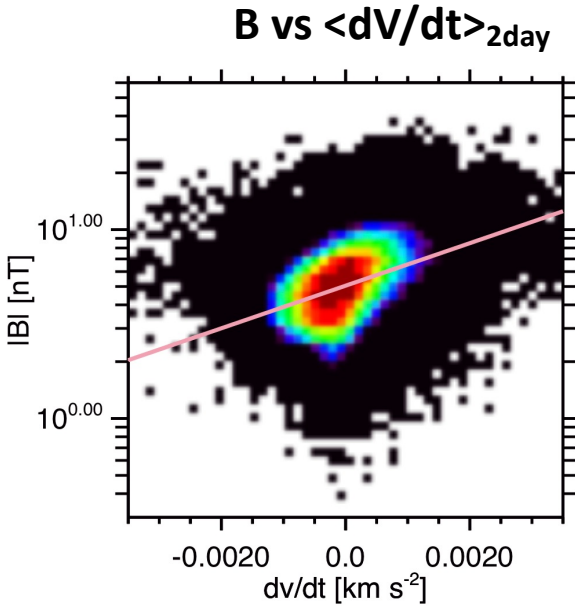

$Y=be^{mx}$
m= 259.4
b= 5.050

Rp=0.406
Rs=0.425

Initial Test Year 2003:
Wide Range of Geoeffective Fast Wind

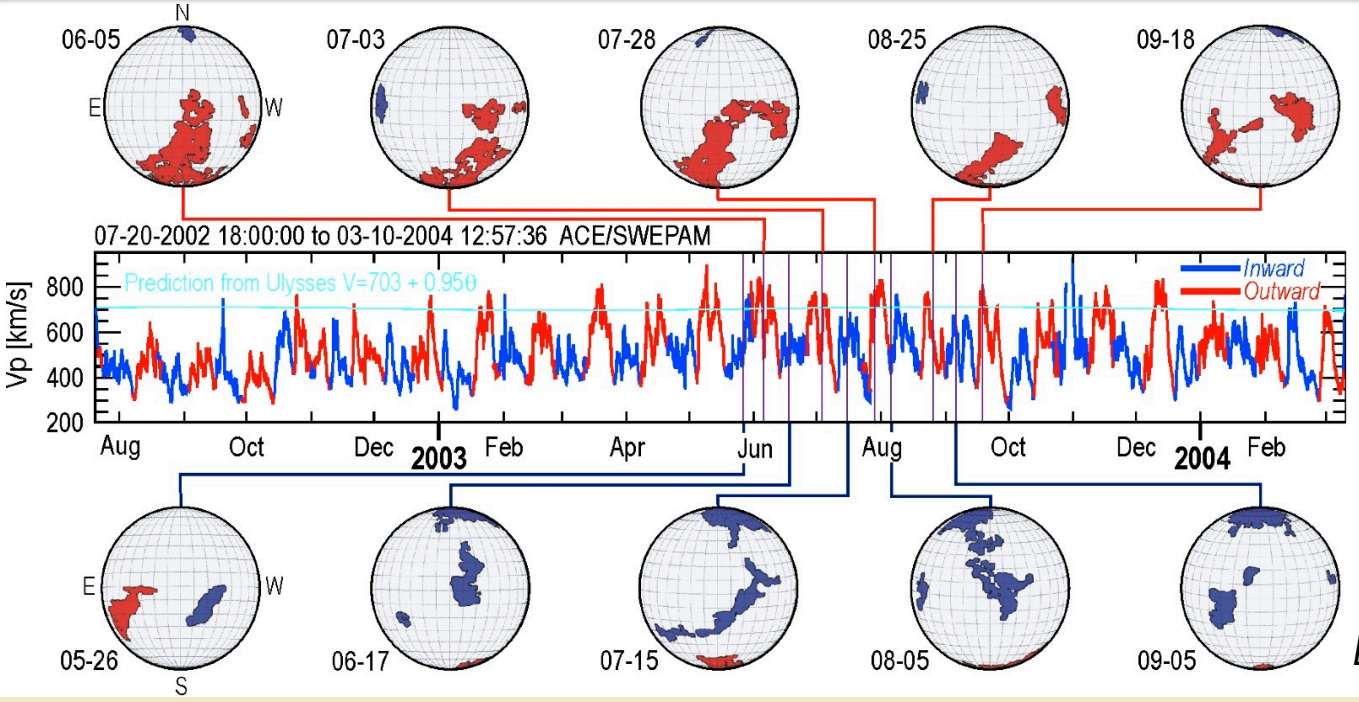

Elliott et al. (2012)

- Year 2003 is an excellent year for testing because there was a long-lived large outward hole and smaller inward polarity holes on the opposite sides of the Sun.
- The wind from the outward polar coronal extension was very geoeffective and more geoeffective than typical equatorial coronal holes.

ADAPT-WSA Solar Wind Speed Time Series Forecast Example

- Solar wind speed time series (**black**) with 3-day lead ADAPT-WSA forecasts over-plotted are (12 realizations **rainbow** colored).
- Bottom panel repeats the solar wind speed data color-coded by polarity.
- Time when there was a very fast polar coronal hole extension (**outward**) and a smaller moderately fast equatorial coronal hole (**inward**) (*Elliott et al., 2012*).

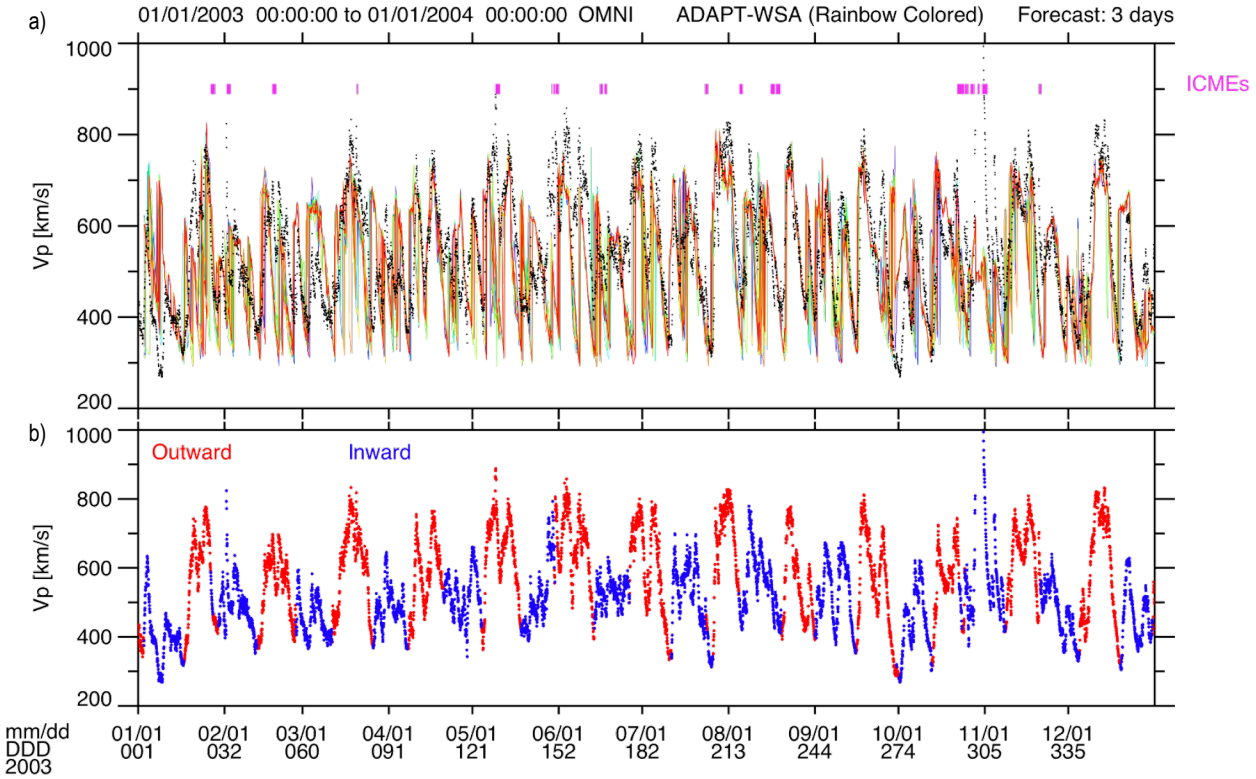

ADAPT-WSA Solar Wind Speed Time Series Forecast Zoom

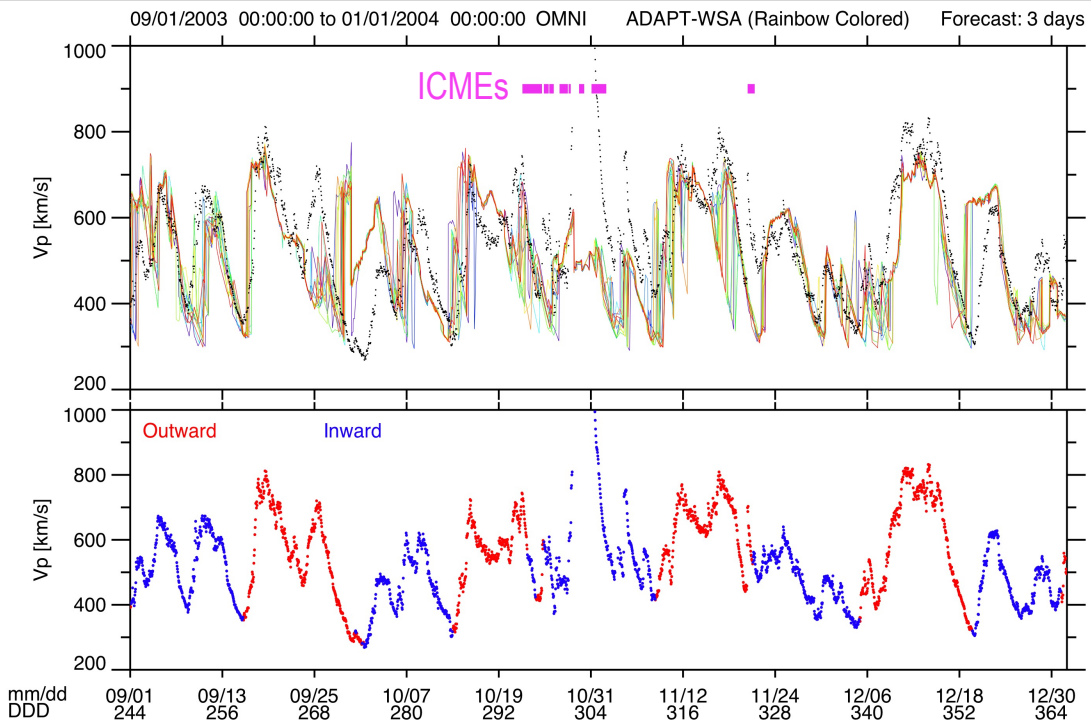

- Solar wind speed time series (black) with 3-day lead ADAPT-WSA forecasts over-plotted are (12 realizations rainbow colored).
- Bottom panel repeats the solar wind speed data color-coded by polarity.
- Time when there was a very fast polar coronal hole extension (outward) and a smaller moderately fast equatorial coronal hole (inward) (*Elliott et al., 2012*).

Kp Index Can Be Forecasted with Using Speed and Density

- 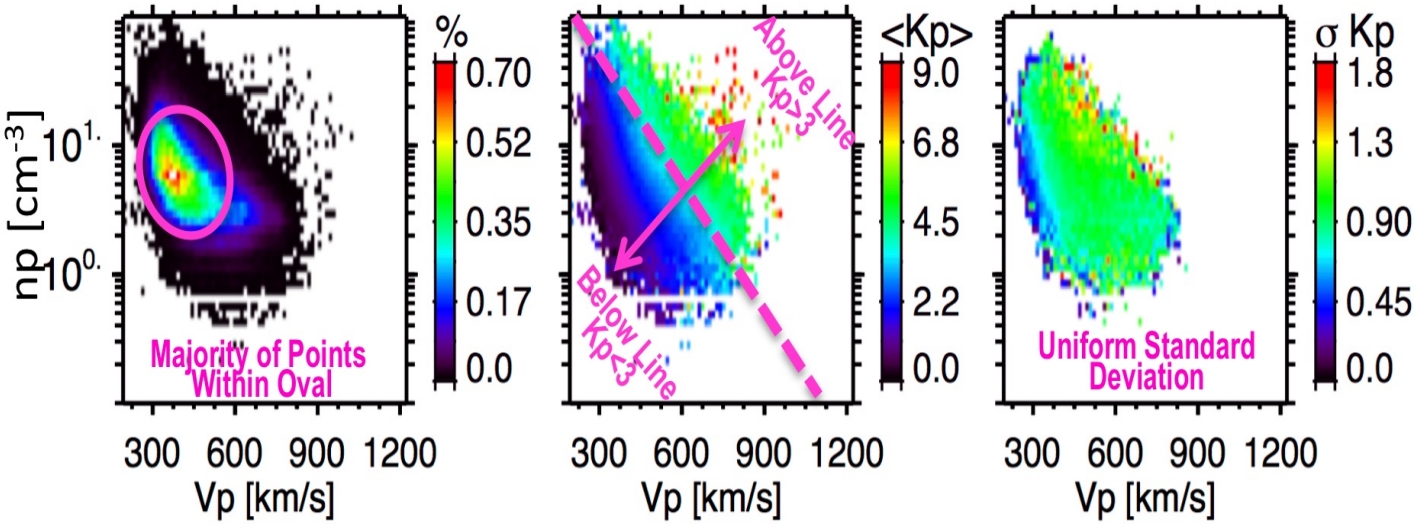

Wang-Sheeley-Arge Speed Formula

$$v_{\mathrm{wsa}}(f_{\mathrm{p}}, d; v_0, v_1, \beta, \gamma, w, \delta) = v_0 + \frac{v_1 - v_0}{(1 + f_{\mathrm{p}})^{\alpha}} \cdot \left\{ \beta - \gamma \cdot \exp[-(d / w)^{\delta}] \right\}^3$$

(Reiss et al., 2019)

Dependent Variables:

- *fp* -expansion factor
- d - angle to the open-closed field line boundary (~ angle to coronal hole boundary)

- All other quantities are coefficients.

ADAPT-WSA Solar Wind Speed Time Series Forecast

- Solar wind speed time series (**black**) with 3-day lead ADAPT-WSA forecasts over-plotted are (12 realizations **rainbow** colored).
- Bottom panel repeats the solar wind speed data color-coded by polarity.
- Time when there was a very fast polar coronal hole extension (**outward**) and a smaller moderately fast equatorial coronal hole (**inward**) (*Elliott et al., 2012*).

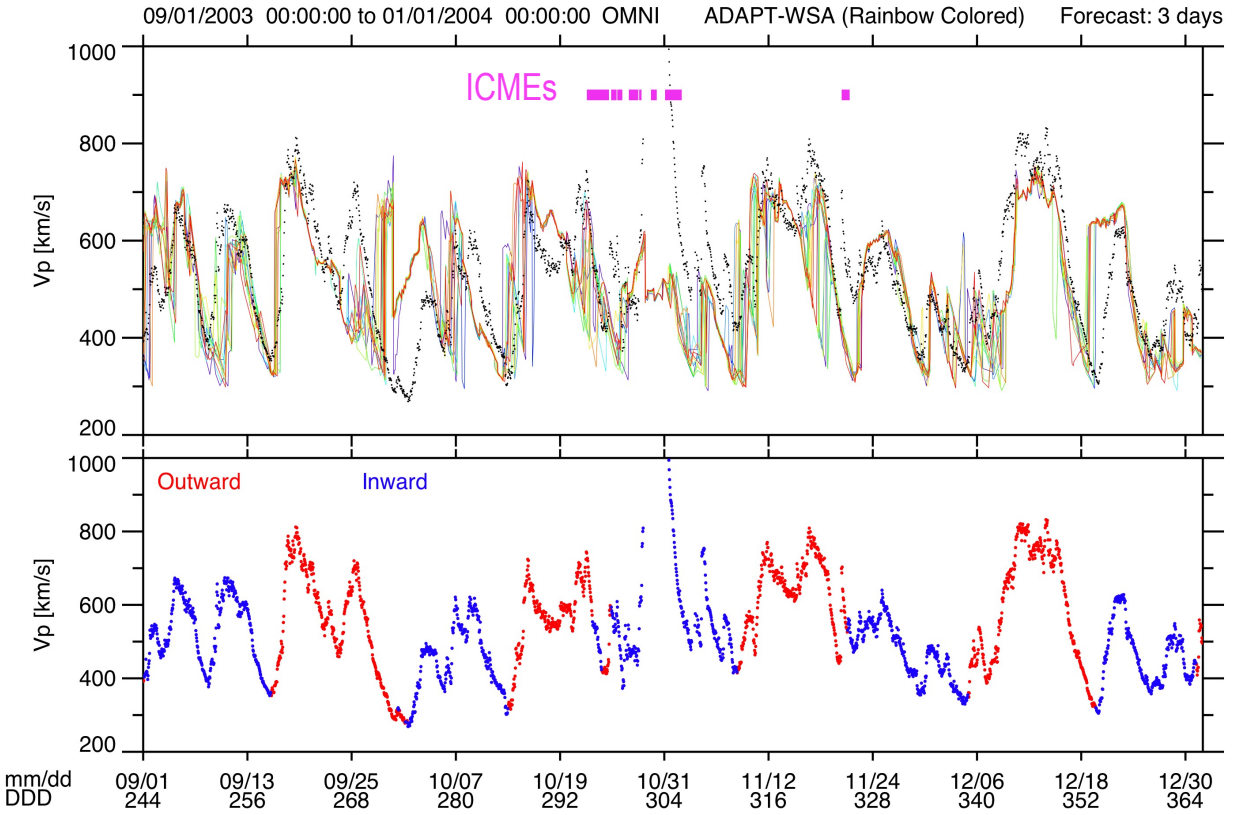

Overview of Residual Errors for ADAPT-WSA 3-Day Speed Forecast

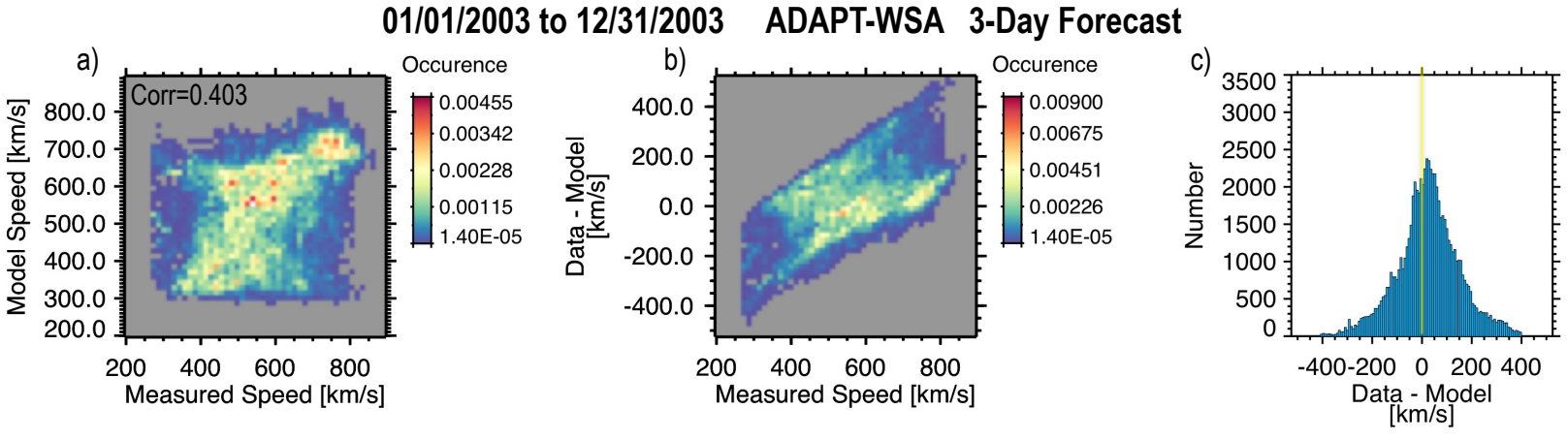

- Left: Direct comparison between model and measured speed.
  The majority of points are along diagonal where the model and measured speeds are equal, but a significant portion are not.
- Middle: Residual error as a function of the measured speed.
  There is a trend in the residual errors with speed.
- Right: Histogram of the residual error.
  The residual error histogram peaks slightly above zero when the model speed is lower than the measured speed.

Speed and Residual Error Dependence on Expansion Factor and Angle to the Boundary

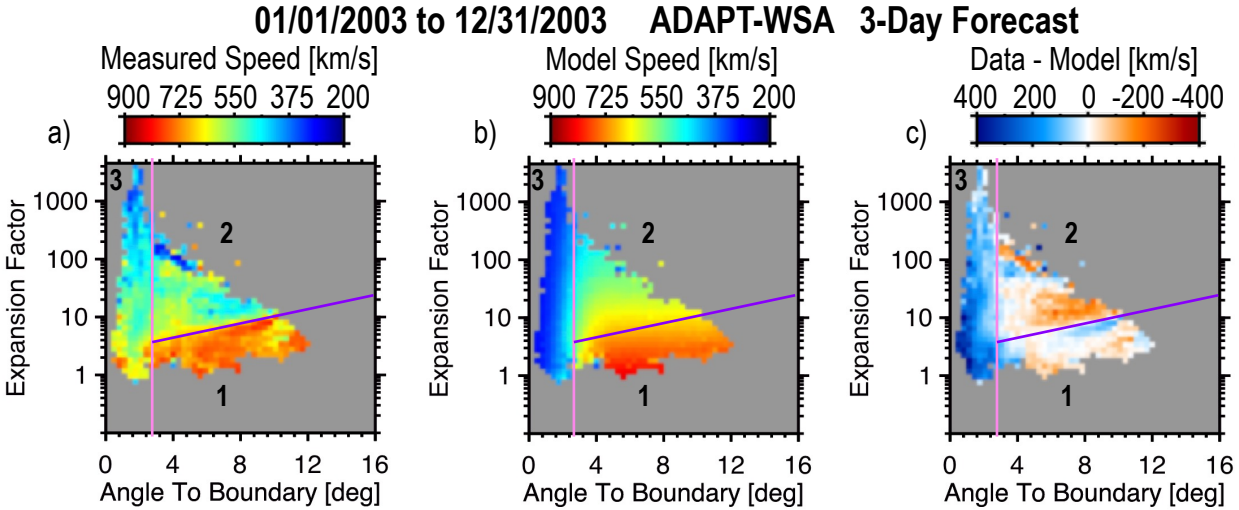

- Left: Data sorted by expansion factor (fp) and angle to the coronal hole boundary (d).
- Middle: ADAPT-WSA 3-Day forecast vs. fp and d (visual representation of WSA formula).
- Right: Residual speed errors vs. fp and d.

Kp Index Can Be Forecasted Using V and n

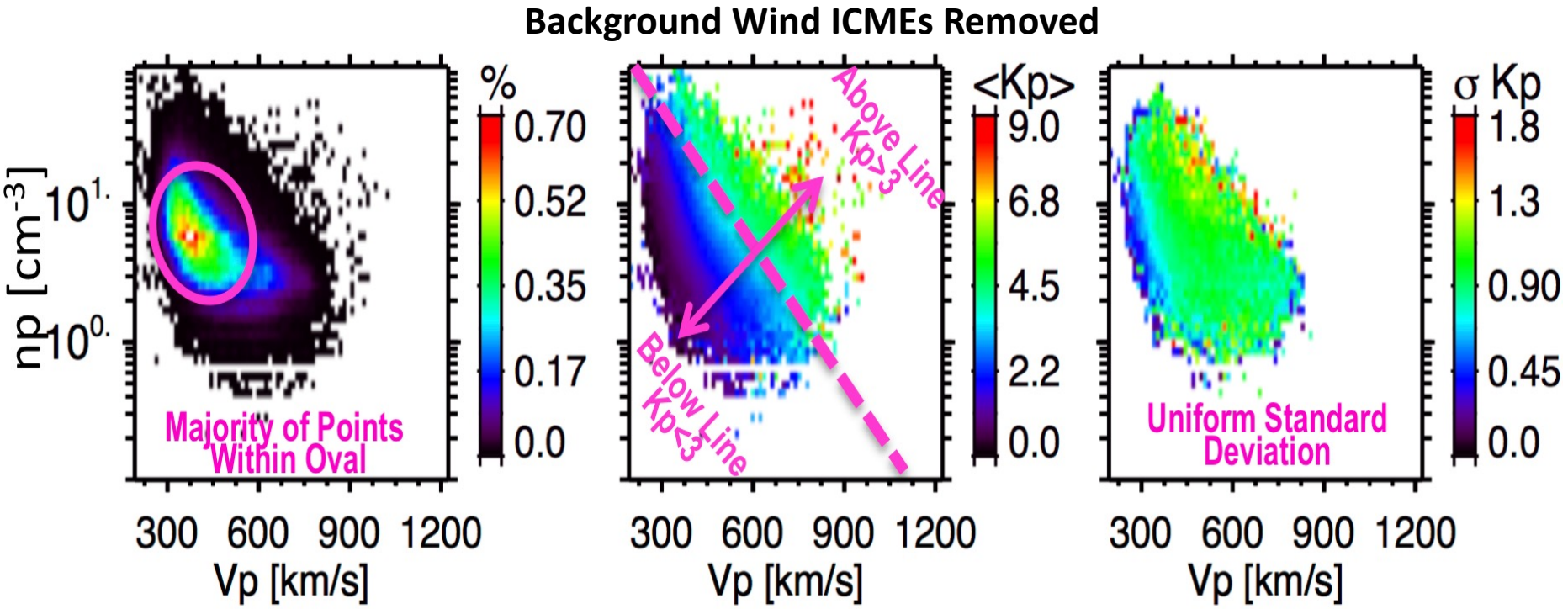

Forecast Test On Full Year (Scalar Quantities)
Using Corrected Speeds and Adjusted Formulas

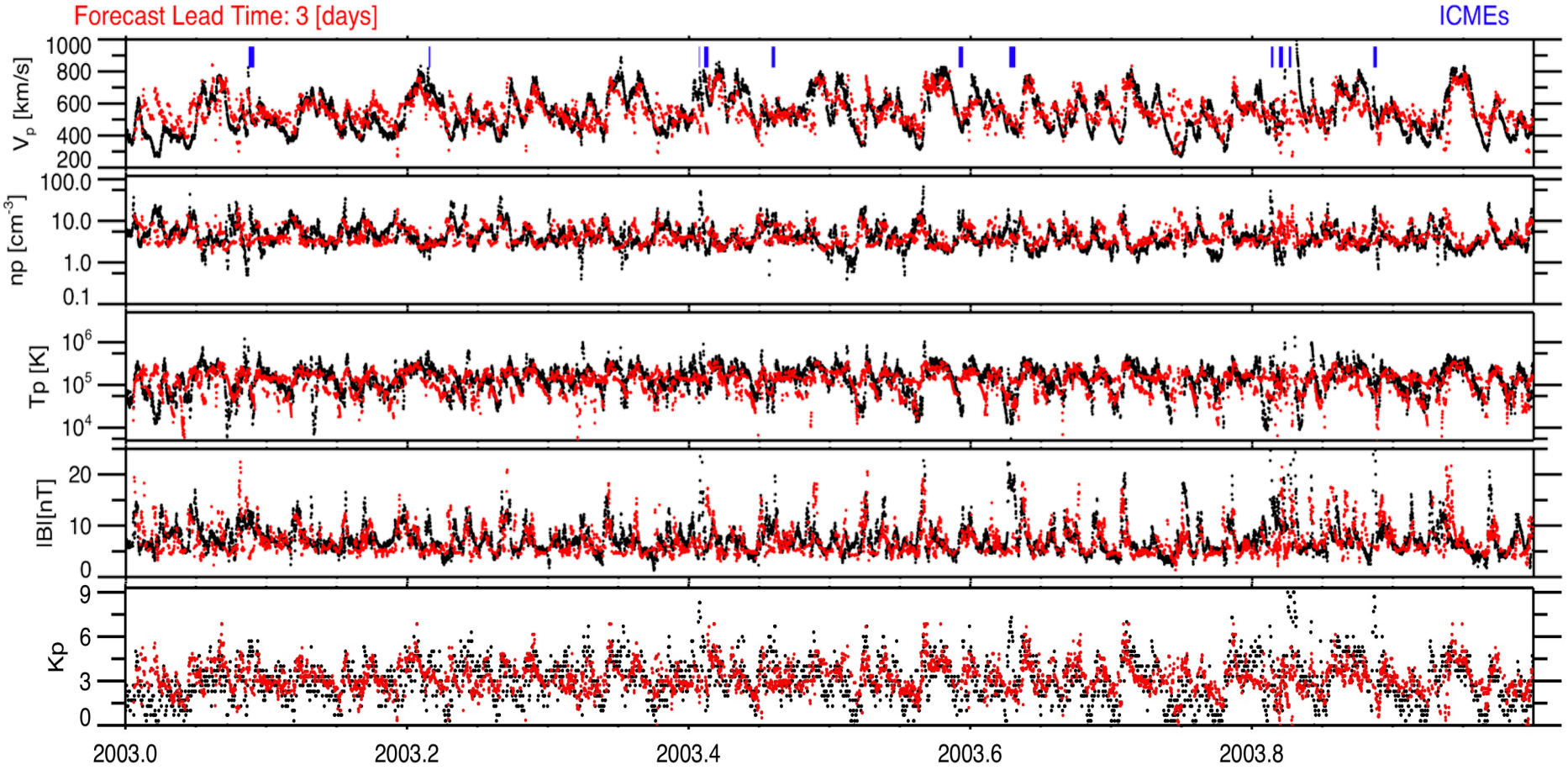

Forecast Test On Full Year (IMF)
Using Corrected Speeds and Adjusted Formulas

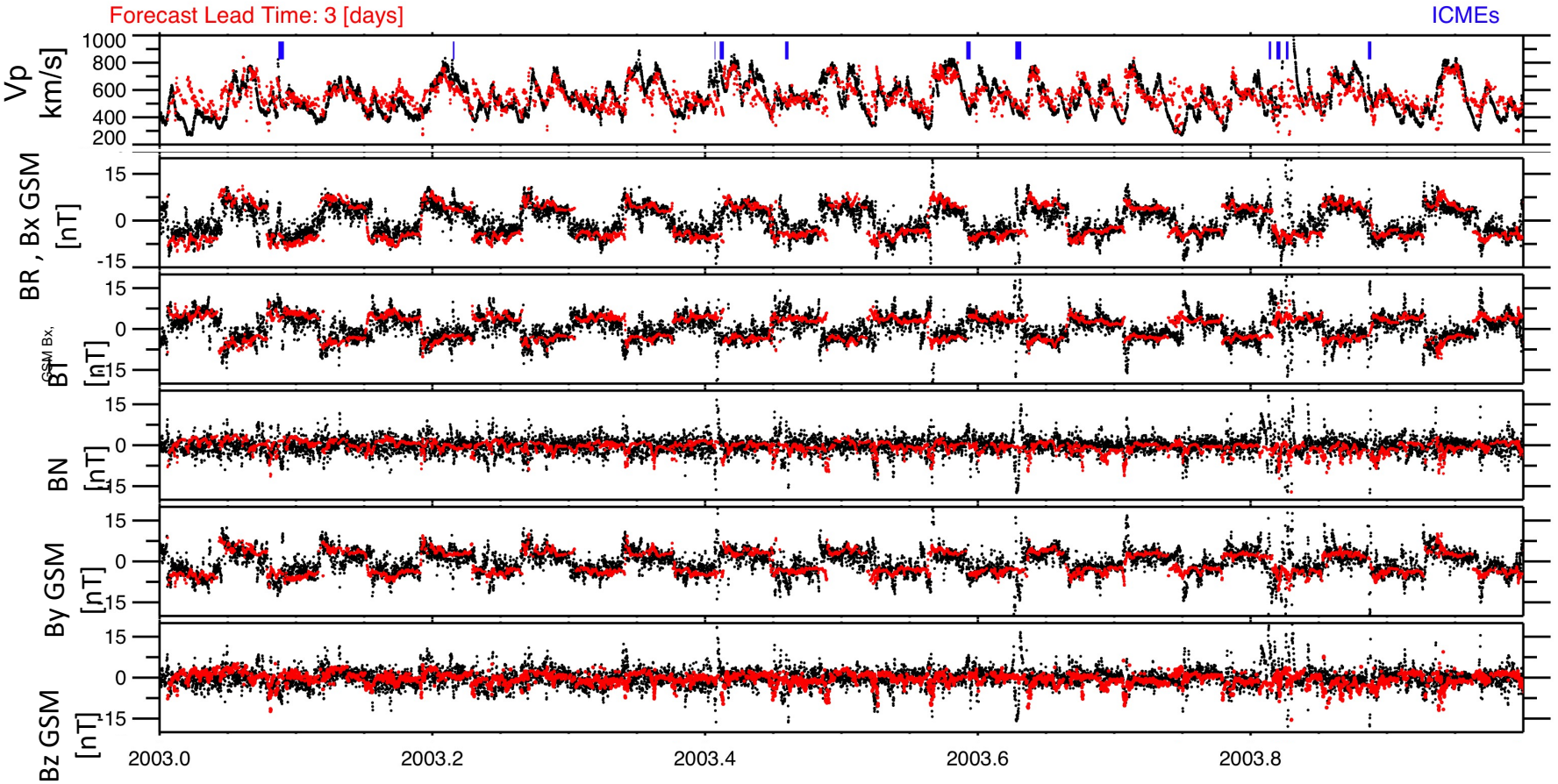

Testing Forecasts of Scalar Quantities

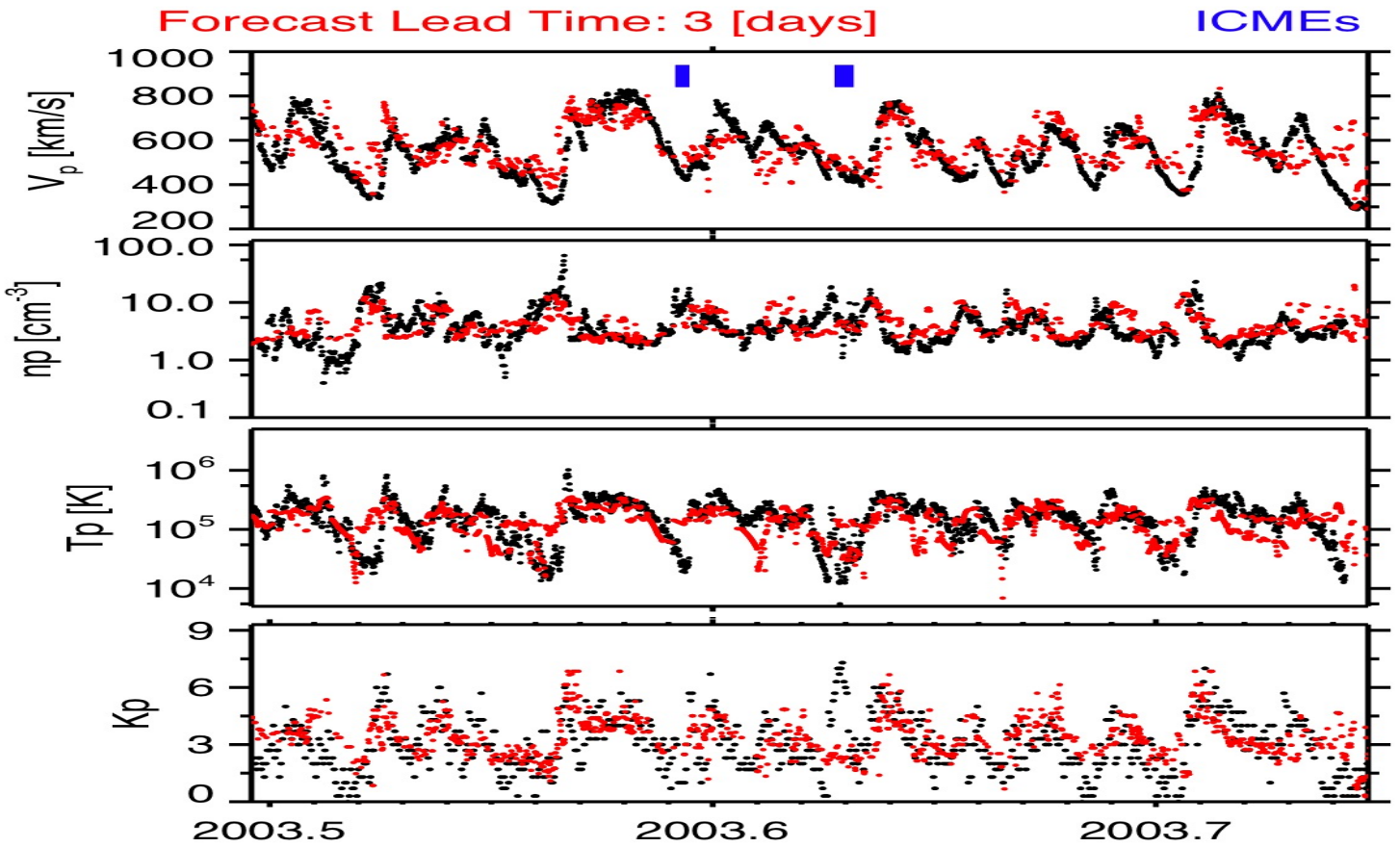

Testing Forecasts of IMF Components

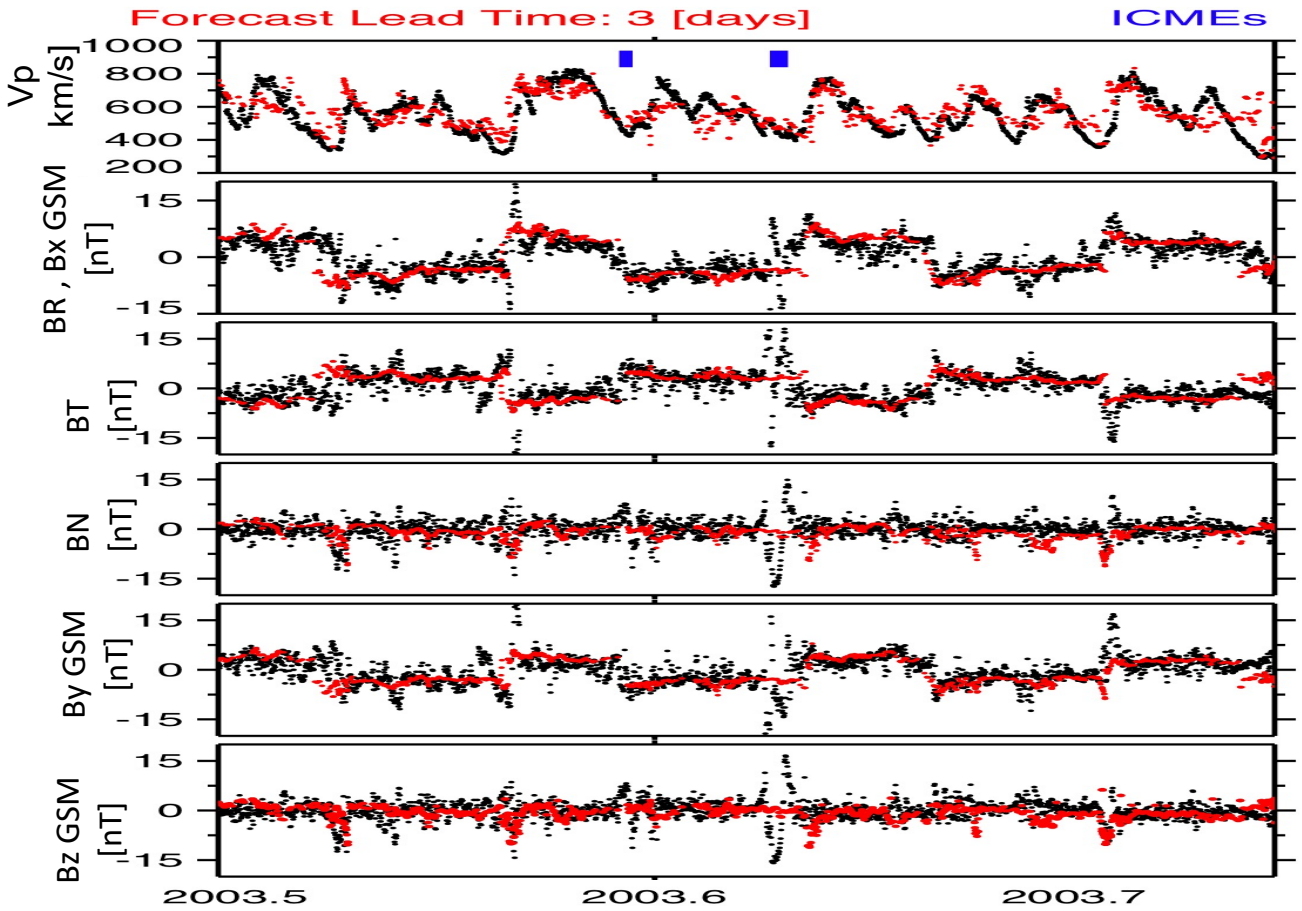

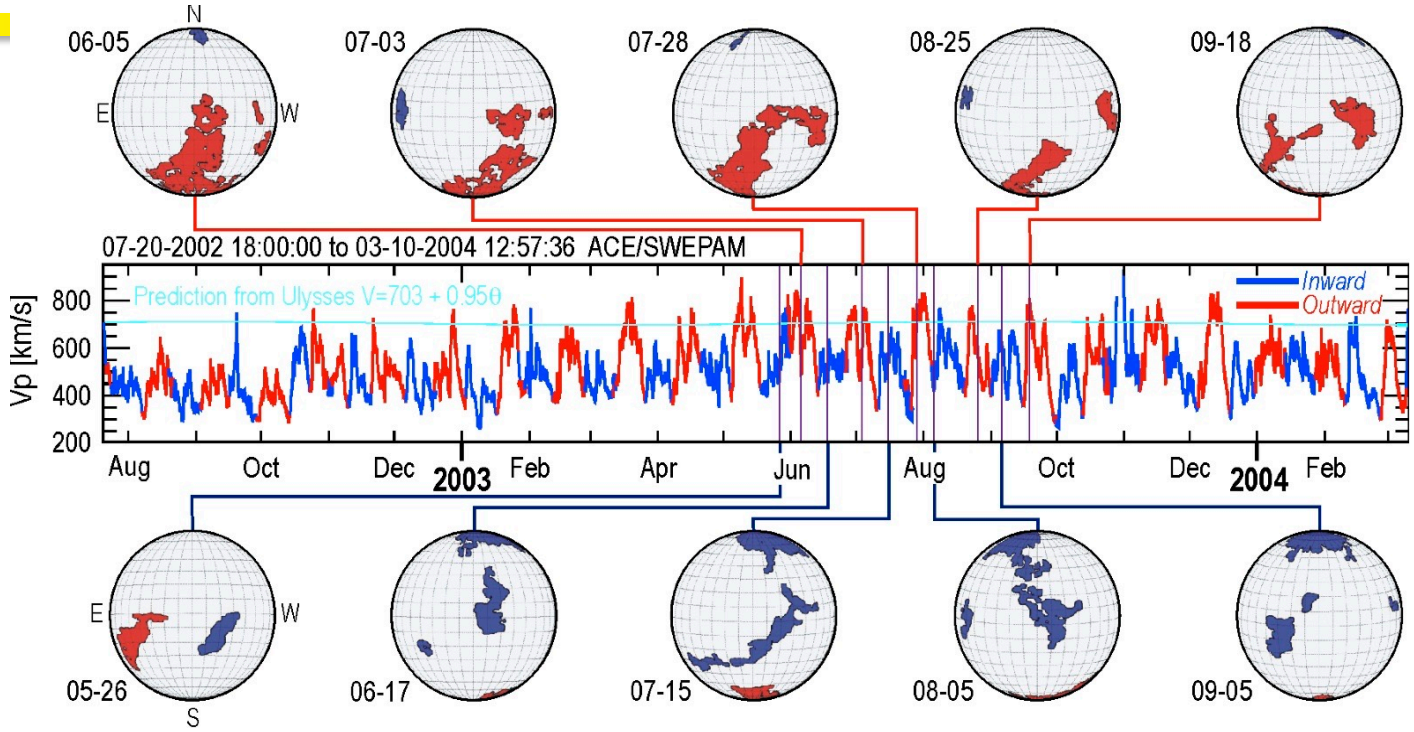

Figure 1: *The top and bottom rows show coronal hole maps with the polarity color-coded. The middle panel shows the solar wind speed measured at ACE at L1 with the polarity color-coded. In 2003 there was a large long-lived outward (red) polarity coronal hole extension that extended from the south pole to low latitudes. On the opposite side of the Sun, there was a smaller low latitude inward (blue) equatorial hole. The outward hole emitted wind with speeds that were similar to the wind speeds above the middle of polar coronal hole. The light blue line shows expected speeds based on a fit of speeds from Ulysses polar coronal hole measurements versus latitude. This figure is from Elliott et al. (2012).*

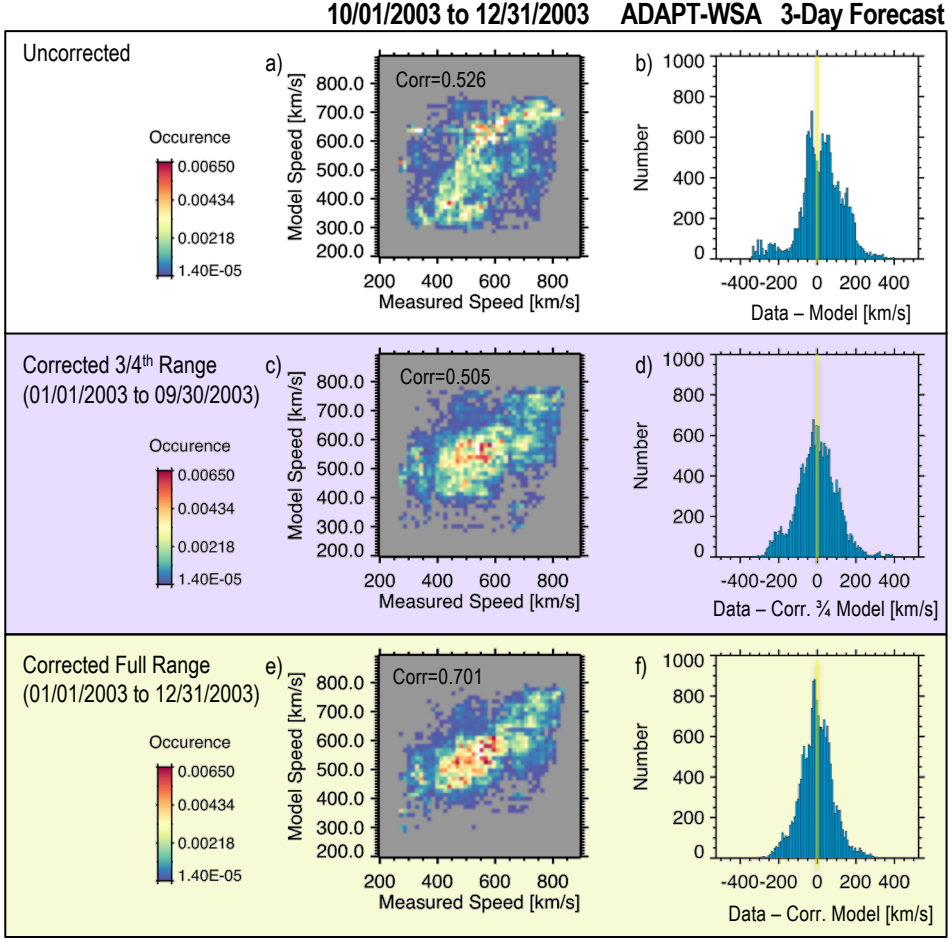

Figure 8: *In the left column are probability of occurrence maps for the model speed versus the measured speed. The Pearson correlation coefficient is listed on each of these plots. Here we examine the time period between October 1, 2003 through the end of December 31, 2003. The right column shows histograms of the absolute error between the data and model. The top row has results ADAPT-WSA without any corrections. In the middle row corrections based on the first 3/4ths of the year (January 1, 2003 through the end of September 30, 2003) are applied, and in the bottom row corrections based on all of 2003 are applied.*

main_evaluate_speed_data-model.pro

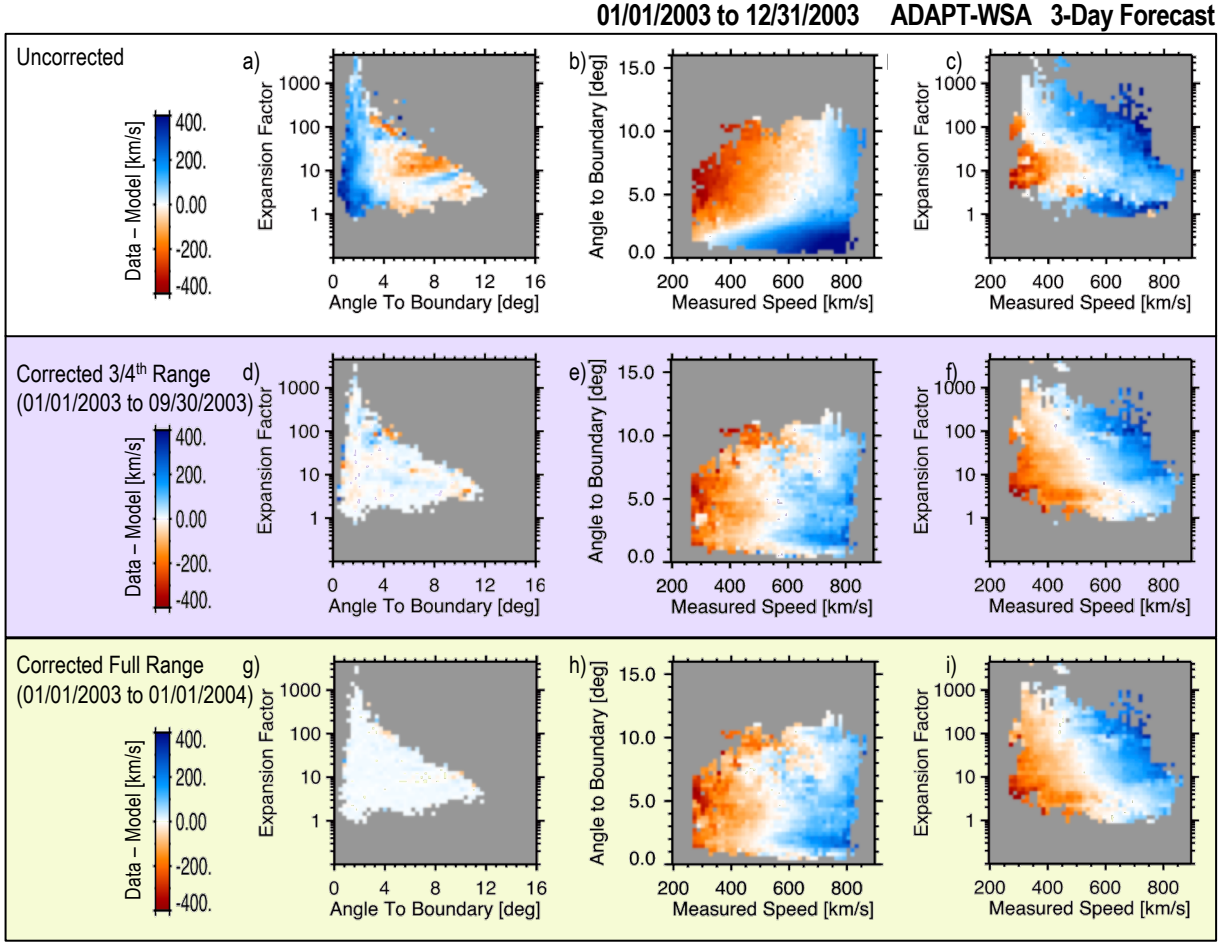

Same plot formats as in
howing the residual
rs as a function of
factor and angle to the
left column), angle to
ry and measured speed
nd expansion factor an
speed (right column).
w has the residual errors
orrected ADAPT-WSA 3
forecasts. The middle
errors when applying
factors based on the
of 2003, and the bottom
the errors when
orrection factors based
003.

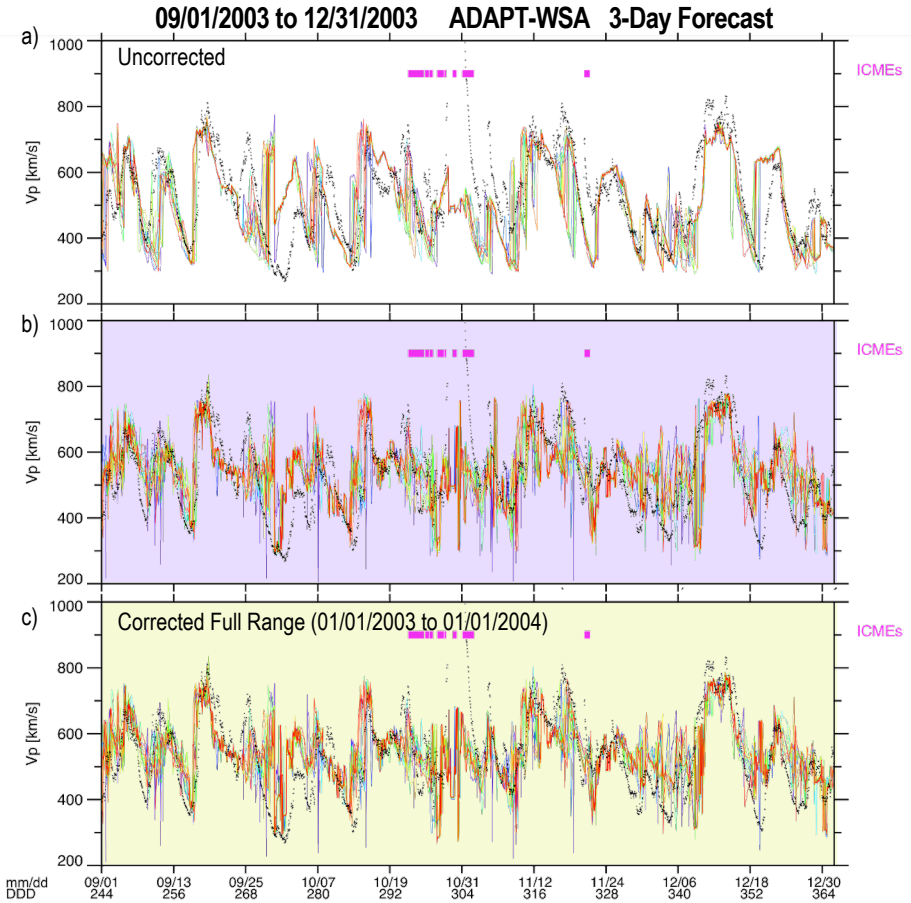

Figure 10: *A 4 month time series plot of the solar wind speed. In the each panel the data are in black and the 3-day forecasts for all 12 realizations are rainbow colored. a) Overlays the uncorrected ADAPT-WSA forecast, b) overlays the corrected forecast based on 3/4ths of 2003, and c) overlays the corrected forecasts based on all of 2003.*

main_wsa_loop_speed_data-model.pro

Determining |B| from dV/dt
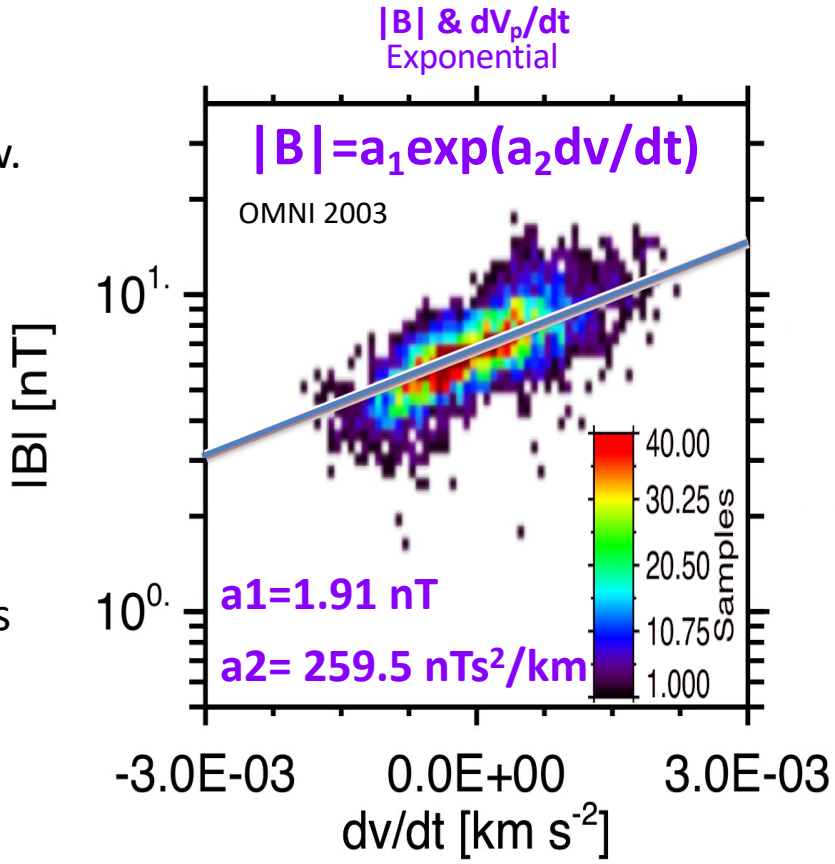
- Compared |B| to the a running estimate of dV(t)/dt in a 2day window.
- The exponential fit parameters for each year of |B| vs. dV/dt do not show a systematic time variation.
- Next we use the fit results for 2003 to estimate the field.